# A CELL-BASED MODEL TO STUDY FACTORS THAT DRIVE DIFFUSE ASTROCYTOMA DEVELOPMENT

Anthony F. Folck

Submitted to the faculty of the University Graduate School
in partial fulfillment of the requirements
of the degree
Master of Science
in the Department of Biochemistry and Molecular Biology,
Indiana University

August 2016

Accepted by the Graduate Faculty, of Indiana University, in partial fulfillment of the requirements for the degree of Master of Science

Master's Thesis Committee

Clark D. Wells, Ph.D., Chair

Mark G. Goebl, Ph.D.

Lawrence A. Quilliam, Ph.D.

## DEDICATION

I would like to dedicate this work to my mother, Beverly, for being an inspiration as she fights her battle, and my father, Chip, for always being a voice of reason during my failure and success.

## ACKNOWLEDGEMENTS

I would like to acknowledge and extend an overarching thank you to Dr. Clark Wells for his support and guidance. Dr. Wells took a chance on me when others wouldn't and helped push me to think, work, and succeed as a scientist.

I would like to thank and acknowledge my committee members Dr. Mark Goebl and Dr. Lawrence Quilliam, as they were invaluable for the support and feedback they provided me throughout my time at Indiana University.

I would like to thank my lab mates Brandon Lane, Kevin Lange, and Lauren Bringman for being a constant source of encouragement and support.

I would like to thank the Indiana University Department of Biochemistry and Molecular Biology for their support and patience throughout this process. Numerous parts of this project would not have been complete without their help. Specifically, Jack Arthur, who always found time to lend a helping hand, whether it was technology related or just a few words of encouragement.

Lastly, I would like to thank my family and friends for their continuous support. I thank my friends for providing me with immeasurable support. I thank my parents for making this possible and providing me with the tools to succeed. Lastly, I thank my sister, Cassie, for always providing me with support, encouragement, and direction, of which I will be ever grateful.

Anthony F. Folck

A Cell-Based Model to Study Factors that Drive Diffuse Astrocytoma Development

Secondary gliomas are an incurable form of brain cancer that are diagnosed in people at a median age of 45 years. Next-generation sequencing has found that secondary glioblastomas have a distinct genetic profile from the more common primary glioblastomas, which are diagnosed in people typically over the age of 60. Over 80% of secondary gliomas contain an $IDH1^{R132H}$ mutation, resulting in neomorphic mutations, which catalyze isocitrate to the oncometabolite D-2-hydroxyglutarate (2-HG) instead of alpha-ketoglutarate (α-KG). As 2-HG accumulates, it induces a hypermethylator phenotype that prevents the cells from differentiating. Acquisition of additional mutations in tumor suppressors such as p53 and/or ATRX likely leads to tumor initiation. Work in the Wells Laboratory has found that loss of the HIPPO adaptor protein AmotL1 is also associated with increased malignancy. AmotL1 inhibits the transcriptional co-activator YAP to suppress both cell growth and migration. To understand the molecular events leading to secondary glioma development, this thesis developed a series of astrocyte cell lines that carry IDH1 and/or p53 mutations. These lines were then studied in 2D and 3D cell culture systems to identify changes that are associated with early secondary glial tumors. Work was also carried out to enable screens for small molecules that can be tested on these cell lines.

Clark Wells, PhD, Chair

**TABLE OF CONTENTS**

## LIST OF TABLES

## LIST OF FIGURES

## ABBREVIATIONS

| | |
|---|---|
| 2-HG | 2-Hydroxyglutarate |
| a-KG | Alpha-Ketoglutarate |
| APC | Astrocyte Precursor Cell |
| ATRX | α-Thalaseemia/Mental-Retardation-Syndrome-X-Linked |
| BCA | Bicinchoninic Acid |
| BME | 2-Mercaptoethanol, 99%, Extra Pure |
| CIMP | CpG Island Methylator Phenotype |
| CTGF | Connective Tissue Growth Factor |
| DNA | Deoxyribonucleic Acid |
| EAAT | Excitatory Amino Acid Transporter |
| ECM | Extracellular Matrix |
| EDTA | Ethylenediaminetetraacetic Acid |
| EHS | Engelbreth-Holm-Swarm |
| DMEN | Dulbecco's Modified Eagle Medium |
| GBM | Glioblastomas Multiforme |
| GFAP | Glial Fibrillary Acidic Protein |
| hEAT | Human Embryonic Astrocyte Tert Immortalized |
| IDH1 | Isocitrate Dehydrogenase 1 |
| IDT | Integrated DNA Technologies |
| MAP-2 | Microtubule-Associated Protein 2 |
| OLIG-2 | Oligodendrocyte Transcription Factor 2 |
| PBS | Phosphate Buffered Saline |

| | |
|---|---|
| PCR | Polymerase Chain Reaction |
| PEI | Polyethylenimine |
| qRT-PCR | Quantitative Real-time Polymerase Chain Reaction |
| RFP | Red Fluorescence Protein |
| SDS-PAGE | Sodium Dodecyl Sulphate-Polyacrylamide Gel Electrophoresis |
| TEAD | TEA Binding Domain |
| TERT | Telomerase Reverse Transcriptase |
| TMZ | Temozolomide |
| TP53 | Tumor Protein 53 |
| WHO | World Health Organization |
| YAP | Yes-associated Protein |

## INTRODUCTION

Gliomas are a broad category of non-neuronal brain cancers that mainly arise from astrocytes, but can also comprise of oligodendrogliomas, ependymomas and mixed lineages. Gliomas are clinically differentiated by histopathologic features into 4 grades that associate with clinical outcomes. Grade I is a noncancerous, slow-growing tumor that has clear margins and can usually be cured with surgery. Grade II-IV tumors diffusely invade into the normal brain, contain a large number of actively dividing tumor cells (hypercellular), and show active angiogenesis. Grade II tumors are distinguished from Grade III tumors by their lack of necrosis (the accumulation of dead cells). Grade IV gliomas, which are often referred to as glioblastomas, are highly invasive and lethal (Aldape et al.).

It is now appreciated that glioblastomas can arise through two very different mechanisms. Glioblastomas that arise from the progression of stages I-III tumors are termed secondary. Conversely, primary glioblastomas are thought to initiate *de novo* as grade IV tumors from neural stem cells (Ohgaki and Kleihues, Reifenberger, 2014 #8). While primary and secondary glioblastomas are histologically indistinguishable, they significantly differ in their age of onset, initial malignancy and genetic and epigenetic profiles (Table 1) (Ohgaki and Kleihues).

Primary glioblastomas account for 45-50% of all primary brain tumors with an annual incidence of ~3 per 100,000 people (Aldape et al., Dolecek, 2012 #7). Primary glioblastomas rapidly develop *de novo* in elderly patients without clinical or histological evidence of a less malignant precursor lesion (Ohgaki and Kleihues). Despite multimodal therapy, including neurosurgical resection and radiotherapy

with concomitant and adjuvant temozolomide (TMZ) (Stupp et al.), the overall prognosis of primary glioblastoma patients remains poor with a median overall survival of 12.5 months (Weller et al.).

Secondary glioblastomas typically arise within the frontal lobe in adult patients (Ferris et al.) as low-grade diffuse astrocytomas that usually take several years to progress to a lethal status (Hegi et al.). Secondary glioblastomas were named based on their rise from the progression of lower-grade gliomas (LGGs) e.g. either grade II or III (Louis et al.). Patients are usually diagnosed at a much younger age with a diffuse glioma (median age of 39 years) where the progression to a secondary glioblastoma can often take 7-10 years. These tumors characteristically have less necrosis than primary glioblastomas (Ohgaki and Kleihues).

The molecular basis for the different natural history of secondary glioblastomas was not understood until large scale sequencing studies in 2008 found that most secondary gliomas contain mutations in the active site of isocitrate dehydrogenase 1 (IDH1) and less frequently IDH2 (Parsons et al.). IDH1/2 mutations are thought to drive tumor initiation, as they are the earliest detectable genetic alteration in precursor low-grade diffuse gliomas (Ohgaki and Kleihues). Further large scale sequencing projects comprising over 1,000 tumors have found that ~80% of all WHO grade II-III diffuse gliomas and secondary glioblastomas have mutations in either IDH1 or IDH2. Approximately 90% of IDH mutations result in an arginine-to-histidine substitution at codon 132 of the IDH1 gene ($IDH1^{R132H}$). The remaining IDH mutations either substitute other amino acids at the R132 position of IDH1 or a Histidine at the R172 residue of the homolog IDH2 (Waitkus, Diplas and

Yan). A mutation of IDH1 or 2 is now agreed to be a definitive diagnostic molecular marker of secondary glioblastoma that is more reliable and objective than clinical or pathologic criteria (Ohgaki and Kleihues).

A shared consequence of the IDH1 mutation is the near-complete elimination of the normal oxidation and decarboxylation of isocitrate to alpha-ketoglutarate (α-KG) (S. Zhao et al.) and the neomorphic overproduction of D-2-hydroxyglutarate (2-HG) via NADPH-mediated reduction of α-KG (Agnihotri, Aldape and Zadeh, Dang, 2009 #6) (Figure 1). The by-product oncometabolite 2-HG is otherwise produced at only modest levels in hypoxic states (Wise et al.). Several studies implicate 2-HG in pro-tumorigenic effects of IDH1 mutants. Metabolite analysis reveals that 2-HG levels are 10-100 fold higher in IDH1 mutated gliomas. Functional studies find that introduction of 2-HG induces epigenomic changes via a CpG island methylator phenotype (CIMP), characterized by increased global DNA methylation. This results in an inhibition of normal differentiation processes, enhanced cell proliferation (Lu et al., Ward, 2010 #35) and has been suggested to block progenitor cells from terminally differentiating (Turcan et al.).

Along with IDH1 mutations, tumor development likely requires inactivation of multiple tumor suppressors (Jiao et al.). Around 65% of diffuse astrocytomas carry a mutant form of p53 and/or ATRX (α-thalassemia/mental-retardation-syndrome-X-linked) (Yan et al.). Mutations in IDH1 likely occur before p53, as low-grade gliomas carry IDH1 mutations without p53 mutations in 17% of cases, whereas p53 mutation occurs without IDH mutations in only 2% of cases. Also, analysis of cases where multiple biopsies were taken from a patient revealed that

IDH1 mutation always occurred before the acquisition of a p53 mutation (Watanabe et al.) (Figure 2). These types of analysis strongly implicate IDH mutations and loss of other tumor suppresses are involved the initiation of secondary gliomas. However, very little is known regarding their proclivity to stay indolent for several years or the changes that occur that drives their progression to a highly malignant status.

To understand factors that may be involved in the progression of secondary gliomas, we analyzed the genes whose transcript levels in The Cancer Genome Atlas (TCGA) analysis of grade II/III gliomas showed a significant association with altered patient survival. This revealed a strong positive correlation between high levels of mRNA for angiomotin family members AmotL1 and AmotL2 with longer patient survival (Figure 3). Further more, patients with IDH1/2 mutations that also had relatively high levels of AmotL1 had a significantly longer survival than those with relatively low levels of AmotL1. This led us to investigate whether AmotL1 may protect patients with IDH1/2 mutations from malignant progression. This was also based on work by several groups, including the Wells' laboratory, that found AmotL1 and AmotL2 bind and regulate apical polarity proteins (Wells et al.) as well as many components in the HIPPO signaling pathway (Adler et al.) to promote the differentation and loss of growth in epithelial cells.

While the HIPPO signaling pathway was initially discovered based on its crucial role in organ size control, it is now well appreciated to relay anti-growth signals from a variety of stimuli including intercellular contacts (B. Zhao et al.). Normal cells cease proliferation upon reaching confluence due to contact with other

cells. Classic studies have found that the loss of contact inhibition is a fundamental property of cancer cells that allows them to form tumors (Hanahan and Weinberg). The HIPPO pathway activates the Large Tumor Suppressor (Lats1/2) kinases in response to metabolic stresses and intercellular contacts. These kinases then phosphorylate and inhbit the transcriptional co-activator Yes-Associated Protein (YAP) (Hao et al.). This prevents YAP from turning on multiple trancription factors in the nucleus that induce pro-growth, survival and invasion programs (B. Zhao et al.). YAP also directly binds and is regulated by Amot family members including AmotL1 and AmotL2. Amots inhibit YAP through sequestration in the cytosol and by inducing YAP degredation. This process depends on the direct phosporylation of the Amot family members by Lats1/2 (Adler et al.) (Figure 4).

Consistent with HIPPO signaling modulating the malignancy of LGGs, our analysis of the TCGA Reverse Phase Protein Array (RPPA) data found an association between increased survival of patients and relatively high levels of phosphorylated-YAP/total YAP. Further, preliminary work by the Wells' Laboratory has shown that expression of $IDH1^{R132H}$ in the glioblastoma cell line, U373MG-(U) results in increased levels of YAP, decreased levels in phospho-YAP, and enhanced YAP dependent transcription of CTGF. These effects were enhanced by AmotL1 silencing and antagonized by AmotL1 overexpression. This suggests that IDH mutations are promoting YAP activity, but are limited by the presence of AmotL1.

Another major unresolved question is the cellular context in which IDH mutations enable glioma formation. In mammalian organ development and maintenance, stem and progenitor cells give rise to each other and to

specialized/differentiated cell types. The equilibrium that governs such plasticity is dictated and sustained by the activities of transcription factors, chromatin regulators, and associated cellular networks (Suva et al.). Increasing evidence suggests that certain tumors depend on the same cellular hierarchy, where sub-populations of cells drive tumor propagation and growth. Coincidentally, transcription factors that direct developmental decisions in the cells can also function as oncogenes by promoting the re-acquisition of developmental programs required for tumorigenesis (Suva, Riggi and Bernstein).

It is believed that human astrocytes exist in two defined functional states: a fetal, highly proliferative astrocyte precursor cell (APC) state and a postnatal, non-proliferative, mature state (Zhang et al.). After proceeding through a maturation process, astrocytes lose their abilities to divide and instead sheath synapses and surround blood vessels to form the blood-brain barrier. Understanding how molecular profiles of human astrocytes mature is critical for mapping brain development and pathologies where astrocytes acquire fetal phenotypes (Zhang et al.). To date, it is poorly understood how deregulation of this process may underlie LGG development. There is strong evidence that stem-like cells drive primary glioblastoma development and growth as well as therapeutic resistance (Bao et al., Chen, 2012 #5). However, it is unclear whether secondary astrocytomas arise from progenitor or adult astrocytes. That study revealed that *TPX2* and *TNC* were only expressed at high levels in APC cells whereas mature astrocytes only expressed high levels of *HSD17B6* and *TLR4* (Zhang et al.) (Table 2).

This current study has developed a series of astrocyte cell lines to study the early events in astrocytoma development. This involved making hTERT immortalized primary progenitor astrocytes that expressed either $IDH1^{R132H}$ alone or in combination with $p53^{R273H}$. Studies were then carried out to define whether these cells lost progenitor status and/or gained features of differentiated adult astrocytes when they were cultured in 3D Matrigel© system. This information will form the basis for future studies to examine how deregulation of HIPPO signaling may then further advance tumorigenic properties that may promote the initiation and/or progression of tumors from such cells.

Table 1. **Primary and Secondary Glioblastomas: Comparison of Clinical Versus Genetic Diagnosis.** Primary Glioblastoma affects a much older population than Secondary Glioblastoma. The presence of the IDH1 mutation is a defined molecular marker in segregating Primary from Secondary (0% vs 100%), followed by mutations in p53 and ATRX. (Table was adapted from Ohgaki, 2013)
[a]Tumors were considered to be primary if the diagnosis of glioblastoma was made at the first biopsy, without clinical or histological evidence of a pre-existing, less malignant precursor lesion, where as the diagnosis of secondary glioblastomas required histological and/or clinical (neuroimaging) evidence of a preceding low-grade or anaplastic astrocytoma.

| | **Primary Glioblastoma** | | **Secondary Glioblastoma** | |
|---|---|---|---|---|
| | **Clinical Criteria[a]** | **Genetic Criteria *(IDH1$^{wt}$)*** | **Clinical Criteria[a]** | **Genetic Criteria *(IDH1$^{mut}$)*** |
| **Fraction in a population** | **94.7%** | **91.2%** | **5.3%** | **8.8%** |
| **Mean age (y)** | **59-62** | **56-61** | **33-45** | **32-48** |
| **Mean clinical history (m)** | **6.3** | **3.9** | **16.8** | **15.2** |
| **Median overall survival (m)** | | | | |
| **Surgery + radiotherapy** | **4.7** | **9.9** | **7.8** | **24** |
| **Surgery + radio/chemotherapy** | | **15** | | **31** |
| **Histologic features** | | | | |
| **Oligodendroglial comp.** | **18%** | **20%** | **42%** | **54%** |
| **Necrosis** | **89%** | **90%** | **63%** | **50%** |
| **Genetic Alterations** | | | | |
| **IDH1 mutations** | **4-7%** | **0%** | **73-88%** | **100%** |
| **p53 mutations** | **17-35%** | **19-27%** | **60-88%** | **76-81%** |
| **ATRX mutations** | **4-7%** | | **57-80%** | |

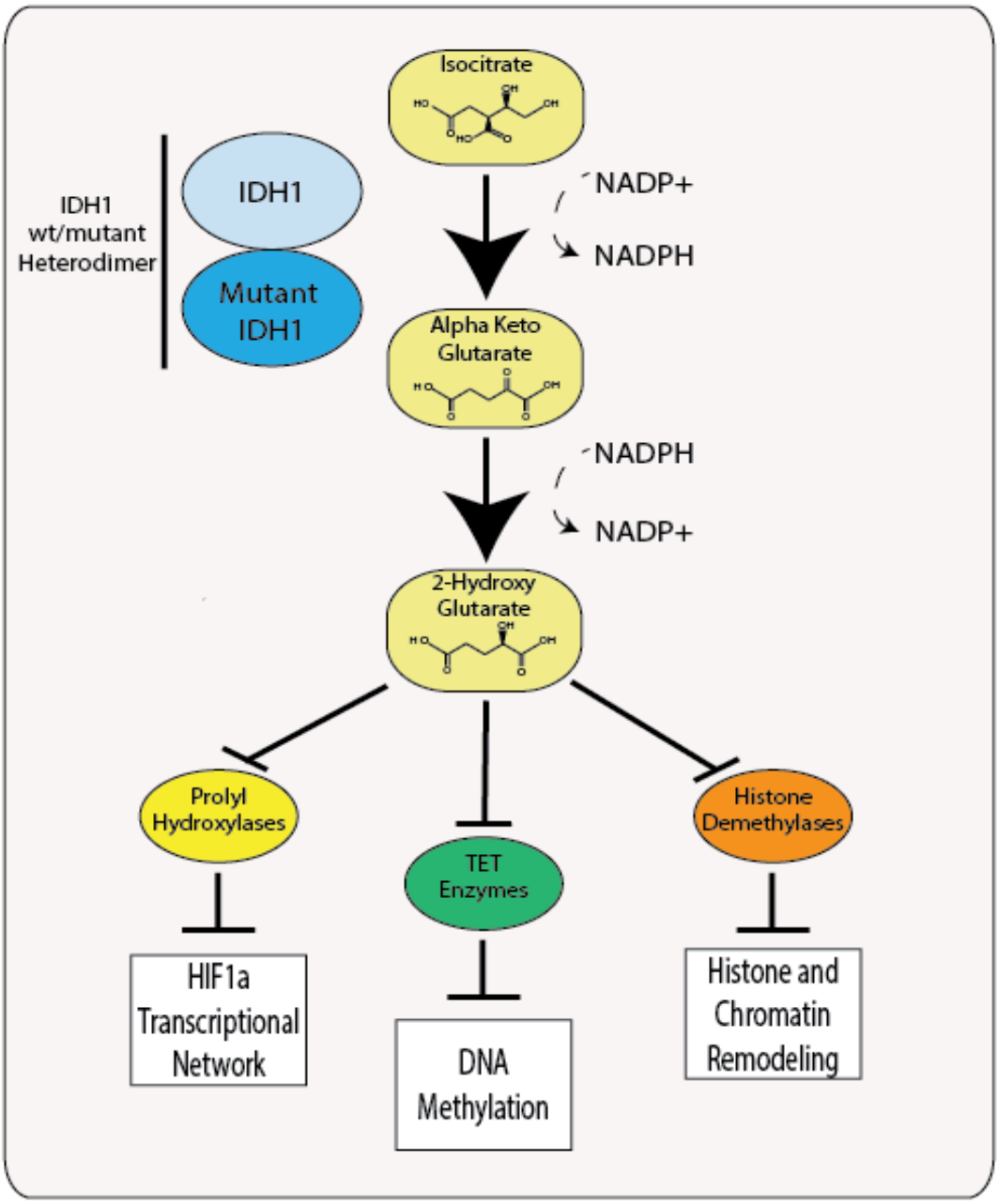


Figure 1. **A Conceptual Model for the Functions of IDH1 Mutations.** IDH1 is a critical member in the Citric Acid Cycle by converting isocitrate to α-KG, which generates ATP for cellular energy. IDH1 mutants are heterozygous and reduce the activity of the wild-type IDH1, resulting in a gain-of-function mutation that produces the oncometabolite 2-HG from α-KG. Overabundant levels of 2-HG result in inhibition of PHD enzymes, TET enzymes, and Histone Demethylases, which leads to a series of detrimental downstream consequences. (Figure was adapted from Agnihotri, 2014)

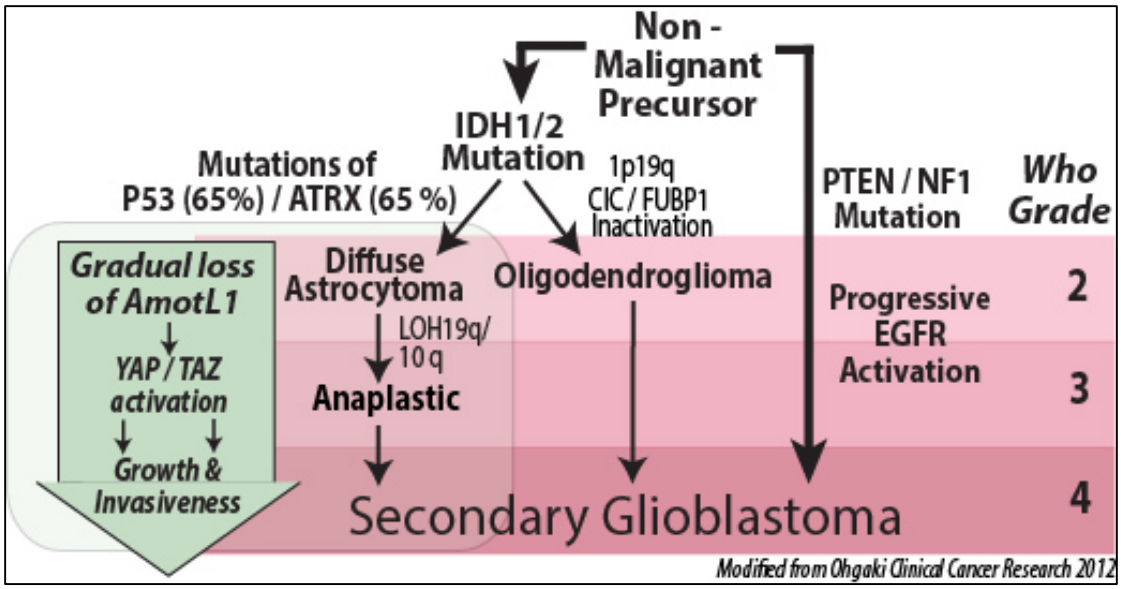


Figure 2. **A Conceptual Model for the Progression of Secondary Glioblastoma.** A series of events must occur for a tumor to progress into malignancy. Secondary Glioblastoma must develop mutations early as a progenitor "precursor" cell, where over time, more mutations will compound. Key mutations include IDH1/2 and p53/ATRX, followed by the gradual loss of AmotL1 and 19q/10q. (Figure was adapted from C. Wells)

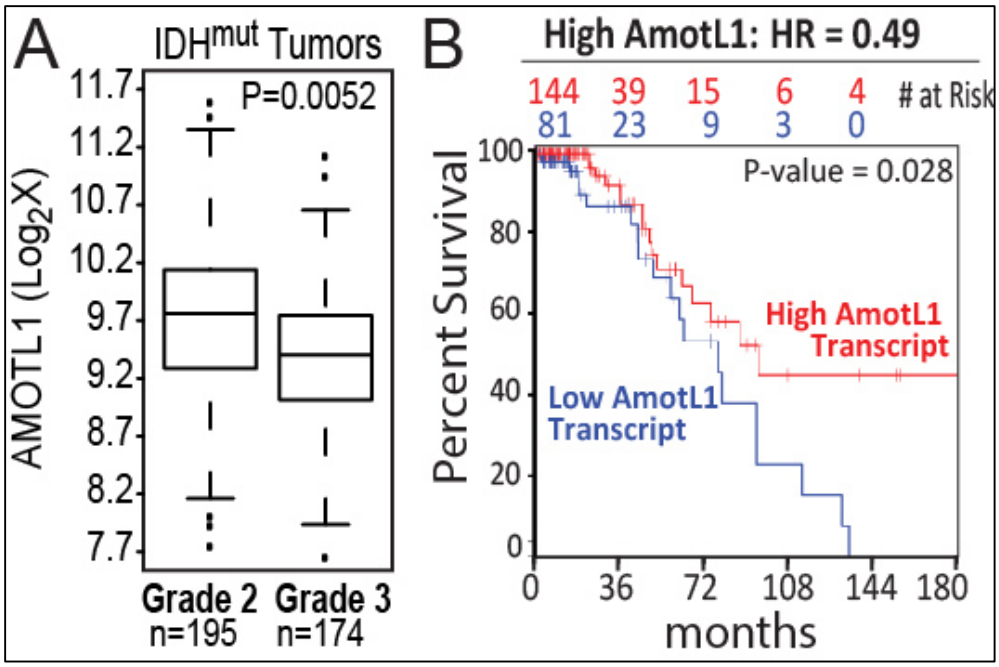


Figure 3. **AmotL1 Expression Correlates With Low Malignancy in IDH$^{mut}$ Gliomas.** A) IDH1/2$^{Mut}$ LGGs in the TCGA were stratified by grade and AmotL1 levels. B) The survival of patients with LGGs in TCGA with IDH1/2$^{Mut}$ were stratified by high or low AmotL1. HR=Hazard Ratio which was computed by Cox proportional Ratio. (Figure was adapted from unpublished data from C. Wells)

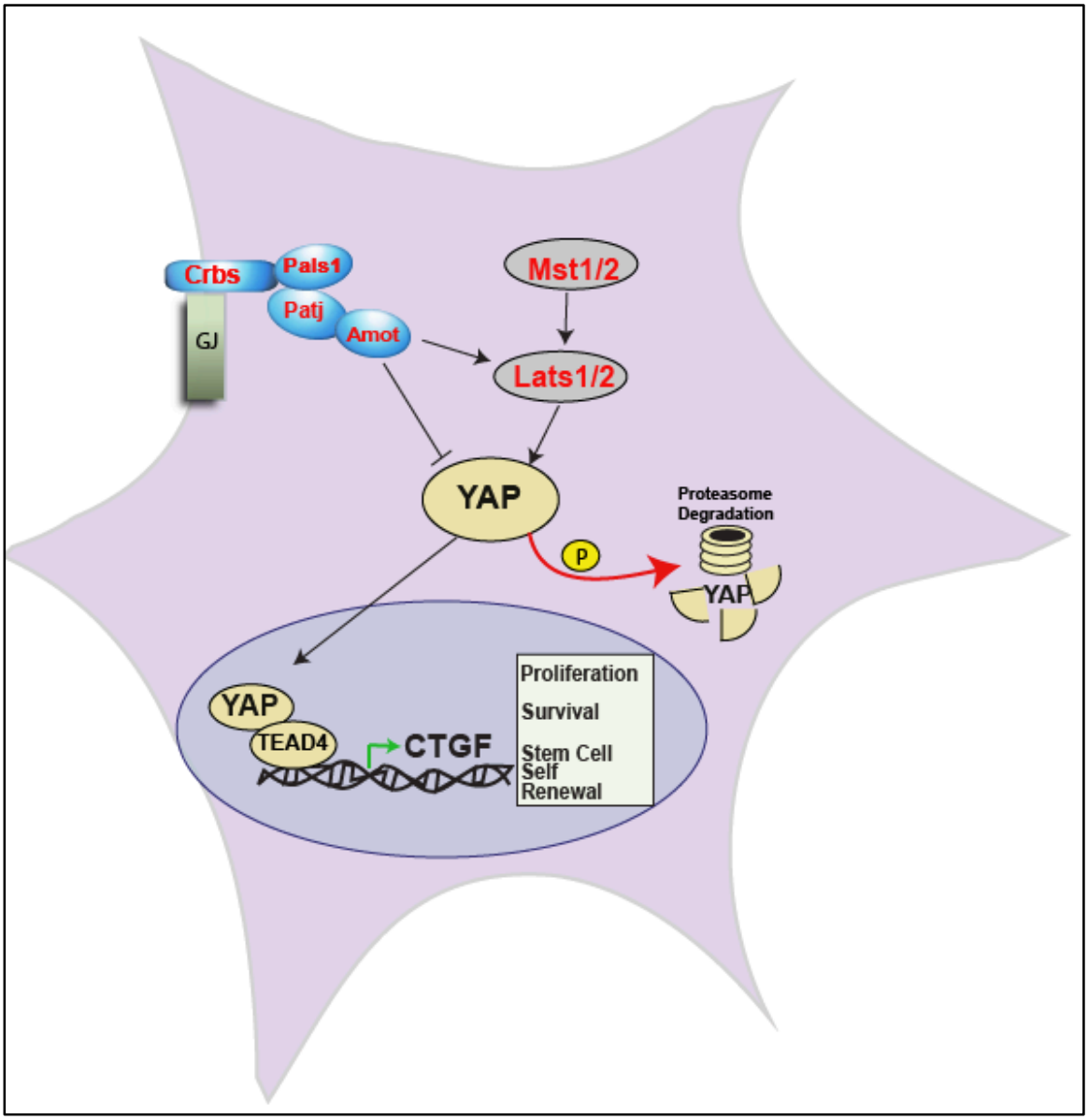


Figure 4. **Overview of the HIPPO Signaling Pathway in the Human Astrocyte.** The transcriptional coactivator YAP is highly regulated by the HIPPO pathway in human astrocytes. Lats1/2 inhibit YAP dependent growth in response to cell-cell contact, by phosphorylating and inactivating YAP, ultimately leading to proteasome degradation via phosphorylation. Alternatively, AmotL1 can inhibit YAP through sequestration techniques and induce proteasome degradation or couple with Lats1/2. If the HIPPO pathway is inactive, YAP is able to localize in the nucleus and interact with TEAD4 to activate transcription factors, ultimately leading to proliferation, survival, and stem cell self renewal.

Table 2. **Top Gene Expression Differences Between APC and Mature Astrocytes** Genes are ranked by fold change in expression between APC and mature stages. Top genes are listed. All genes have >2-fold enrichment in astrocytes over other cell types. (Table was adapted from Barres, 2016)

| Gene | Expression in Fetal Astrocytes | Expression in Mature Astrocytes | Fold Change |
|---|---|---|---|
| **Top Mature Astrocyte Genes** | | | |
| AGXT2L1 | 0.1 | 238.6 | 1,988.6 |
| S100A1 | 0.1 | 84.9 | 849.4 |
| SLC14A1 | 0.1 | 29.3 | 334.6 |
| *TLR4 | 0.1 | 18.7 | 212.9 |
| *HSD17B6 | 0.1 | 20.5 | 204.6 |
| **Top APC Genes** | | | |
| HIST1H2AI | 57.9 | 0.1 | 578.9 |
| HIST1H3E | 51.0 | 0.1 | 509.6 |
| *TPX2 | 22.0 | 0.2 | 93.9 |
| *TNC | 26.6 | 0.6 | 45.5 |
| E2F5 | 10.1 | 1.4 | 7.0 |

*Genes used in qRT-PCR for expression change experimentation

## MATERIALS AND METHODS

### *IDH1 R132H Mutant Cloning*

Human IDH1 R132H was purchased as a gBlock® Gene Fragment (#132285073) from Integrated DNA Technologies (IDT). Preparation of mCherry tagged (V3610) and 3X Flag (V3409) lentiviral vector: 1 µg of vector was linearized by restriction digest in 20 ul with the restriction endonucleases Asc1 and Pac1. The 5' phosphates were removed from the vector with 1 µl of alkaline phosphatase and digested for 15 minutes at 37°C. The samples were then isolated via gel electrophoresis and purified using Qiagen® Qiaex® II Gel Extraction Kit (#20051). The gBlock® DNA gene fragments were suspended in 20 µl TE (10 mM Tris, 0.1 mM EDTA, pH 7.5). 10 µl of the suspension was used in a 20 ul digestion with the Asc1 and Pac1 restriction endonucleases. The gBlock® digestion was heated at 37°C for 150 minutes, then heat inactivated at 70°C. A ligation using 50 ng vector and 20 ng digested gBlock® gene fragment was carried out with T4 DNA ligase buffer (diluted to 1X) and 400 U T4 DNA ligase, for a total volume of 20 µl for 2 hours at 16°C. One tenth (2 µl) of the ligation reaction was then transformed into chemically competent DH5 alpha cells. The transformed bacteria were grown on an ampicillin resistant agar plate overnight, developing individual colonies. These colonies were picked and grown in 1x LB and 1X Ampicillin (100 ug/ml) for 16 hours at 37°C. They were then miniprepped and test digested for validation.

IDH1 R132H gBlock® Sequence (R132H mutation is bold and underlined): 5' -
CCAGGGTTTCTTTGGAATTATTCATACTTATCCTGTCCCTTTTTTTTCCCCAGGGGCGCG

CCTCCAAAAAAATCAGTGGCGGTTCTGTGGTAGAGATGCAAGGAGATGAAATGACACGA
ATCATTTGGGAATTGATTAAAGAGAAACTCATTTTTCCCTACGTGGAATTGGATCTACA
TAGCTATGATTTAGGCATAGAGAATCGTGATGCCACCAACGACCAAGTCACCAAGGATG
CTGCAGAAGCTATAAAGAAGCATAATGTTGGCGTCAAATGTGCCACTATCACTCCTGATG
AGAAGAGGGTTGAGGAGTTCAAGTTGAAACAAATGTGGAAATCACCAAATGGCACCATA
CGAAATATTCTGGGTGGCACGGTCTTCAGAGAAGCCATTATCTGCAAAAATATCCCCCGG
CTTGTGAGTGGATGGGTAAAACCTATCATCATAGGT**CAC**CATGCTTATGGGGATCAATC
AGAGCAACTGATTTTGTTGTTCCTGGGCCTGGAAAAGTAGAGATAACCTACACACCAAG
TGACGGAACCCAAAAGGTGACATACCTGGTACATAACTTTGAAGAAGGTGGTGGTGTTG
CCATGGGGATGTATAATCAAGATAAGTCAATTGAAGATTTTGCACACAGTTCCTTCCAA
ATGGCTCTGTCTAAGGGTTGGCCTTTGTATCTGAGCACCAAAAACACTATTCTGAAGAAA
TATGATGGGCGTTTTAAAGACATCTTTCAGGAGATATATGACAAGCAGTACAAGTCCCA
GTTTGAAGCTCAAAAGATCTGGTATGAGCATAGGCTCATCGACGACATGGTGGCCCAAGC
TATGAAATCAGAGGGAGGCTTCATCTGGGCCTGTAAAAACTATGATGGTGACGTGCAGT
CGGACTCTGTGGCCCAAGGGTATGGCTCTCTCGGCATGATGACCAGCGTGCTGGTTTGTC
CAGATGGCAAGACAGTAGAAGCAGAGGCTGCCCACGGGACTGTAACCCGTCACTACCGCA
TGTAACCAGAAAGGACA - 3’

***P53 R273H Mutant Cloning***

A complete pLenti6/V5-p53_R273H construct was order and received from Addgene (Plasmid #22934). The p53 R273H gene was PCR amplified using the primers O2609 (ACGTGGCGCGCCGAGGAGCCGCAGTCAGATCCTAGC) and O2610 (ACGTTTAATTAATCAGTCTGAGTCAGGCCCTTCTG). The PCR product was gel

purified and then digested with Asc1 and Pac1. This was then gel purified again and ligated into the mCherry tagged lentiviral vector (V3610) with restriction enzymes Asc1 and Pac1.

***TEAD1 Cloning***

A full-length version of TEAD1 (V3441) was cut with Asc1 and Mfe1 restriction enzymes to truncate the front 80 base pairs in order to replace it with a synthesized gBlock® gene fragment from Addgene (O2594), using the same protocol as above.

***TEAD4 Cloning***

A smaller manipulated version of TEAD4 was amplified out of the p-GEX-6p-1 construct using forward primer 144932201 (TEAD MG Vector_F -- ATATAGATCTATGCAGGACCCGGACACGTACAAC) and reverse primer 144932202 (TEAD MG Vector_R – ATATAAGCTTTCATTCTTTCACCAGCCTGTAG) with the phusion enzyme. It was then loaded in a 0.8% agarose gel and run out for 45 minutes at 100 volts. The band was extracted, purified, and digested with HindIII and BglII enzymes. It was once again run on a 0.8% agarose gel and purified. The Pet28a (+) vector was received from the Georgiadis Laboratory at the Indiana University School of Medicine and digested with HindIII and BamH1. The vector was then gel purified and ligated using T4 ligase with the TEAD4 insert overnight. The constructs were then transformed onto a kanamycin resistant plate and grown at 37°C overnight. The colonies grew and were inoculated overnight in 1x LB and 50

ug/ml Kanamycin at 37°C. The inoculations were miniprepped and validated by restriction digest and gel electrophoresis. The samples were finally sent for sequencing using T7 and T7-Term primers. Once validated, the constructs were given to the Georgiadis Laboratory for further experimentation.

***Cell Line and Culturing***

Human Embryonic Astrocyte TERT Immortalized (hEAT) cells were purchased from Applied Biological Materials Inc. labeled as cell line T0281. They were passaged at 37°C with 5% $CO_2$ on 10 $cm^2$ dishes in Prigrow IV Medium supplemented with 10% Fetal Bovine Serum (FBS) and 5 ml of Penicillin/Streptomycin. Once plates were confluent, growth media was aspirated and cells were washed with 1x PBS and then detached from the plate by adding 1 ml of trypsin supplemented with 5 mM ethylenediaminetetraacetic acid (EDTA). After ~10 minutes of incubation at 37°C, adding 3 ml of Dulbecco's Modified Eagle Medium (DMEM) supplemented with 10% FBS and 5 ml of Penicillin/Streptomycin quenched the reaction and the combination was transferred to 15 ml conical tubes. These tubes were centrifuged at 1500 RPM for 1.5 minutes, and the media was aspirated. The pellet of cells was suspended in complete Prigrow IV and split into assays after being counted on a hematocytometer. hEAT cell lines were created in four separate conditions: RFP Control, $IDH1^{R132H}$, $IDH1^{R132H}$ + $p53^{R273H}$, and $p53^{R273H}$ alone.

### *Growth Assays*

Growth assays were completed by plating 150,000 cells with 150 µl of a reconstituted, lamin-rich, basement membrane (Matrigel©) and grown for 24-96 hours at 37°C. Images were acquired on the 1500Z Nikon Stereoscope.

### *Viral Transfection*

In 1 ml of serum-free media the following transfection mixture was prepared: 20 µg of target cDNA, 10 µg pRRE and pRSV-REV, and 6 µg VSVG. 25 µl of polyethylenimine (PEI) (2 µg/ml) was then added to the mixture while being vortexed. Mixtures were incubated at room temperature for 5 minutes and added drop wise to a 10 $cm^2$ plate that was seeded with 4 million 293T cells. Finally, viral media was collected every 24 hours, spun down, and transferred to a new 15 ml conical tube. Collection was completed for a total of 48 hours.

### *Viral Infection*

24 hours prior to viral infection, hEAT cells were approximately 90% confluent on a 10 $cm^2$ plate, were trypsinized, spun down at 1500 RPM, and re-seeded on 6 $cm^2$ dishes at a count of 250,000 cells/dish. After 24 hours, growth medium was aspirated and dishes were incubated for 4-6 hours with viral media that was diluted anywhere from 1:2 – 1:12 in complete DMEM, depending on the virus. Finally, viral media was aspirated and cells were again cultured in complete media for 24 hours at 37°C.

***DNA/RNA/Protein Extraction***

hEAT cells were plated in 10 $cm^2$ at 500,000 cells per plate, per condition, in 10 mL of complete Prigrow IV media. They were grown to ~95% confluence in biological triplicate. The DNA, RNA, and Protein were extracted following a modified version of the Qiagen® AllPrep® protocol and kit. Cells were harvested from plates with 1 mL of 1x PBS and transferred to a 1.5 mL microcentrifuge tube. The cells were spun at 7800 RPM for 5 minutes at 4°C. The PBS was aspirated and 600 ul of RLTplus with 1% 2-Mercaptoethanol, 99%, extra pure (BME) was added. The RLTplus was only added to one of the three tubes per condition, where it was suspended, combined with the next tube, suspended, and recombined with the third replicate tube. The tubes were then raked across a rack 10 times, twice in a minute. The vortexed solution was homogenized with a 23G needle and syringe by pipetting up and down 10 times. After homogenizing, the solution was spun through an AP-DNA column at 9100 RPM for 60 seconds at room temperature. The DNA is bound to the column and transferred to a new AP-DNA column while the flow-thru was combined with 900 µl of 100% ethanol (ETOH). This ETOH/RNA/Protein solution was loaded and spun through an RNeasy column at 10,000 RPM for 30 seconds, where the RNA was bound to the column and the protein was collected and stored in 1.5 mL microcentrifuge tubes. The RNA column was next washed with 700 µl of RWT buffer and spun at 10,000 RPM for 30 seconds. The DNA column was then washed with 500 µl AW1, while the RNA column was washed with 500 µl RPE, both spun at 10,000 RPM for 30 seconds. The flow-throughs were discarded and the DNA and RNA columns were washed again with 500 µl of AW2 and 80% ETOH,

respectively, for 13,300 RPM for 5 minutes. Both DNA and RNA columns were placed into new 1.5 mL microcentrifuge tubes and spun at 13,300 RPM for 15 minutes to dry and eliminate the solvent peak. After the spin, they were left in the hood for 5 minutes to air dry. The RNA column was eluted with 100 µl of DI water and spun at 13,300 RPM for 1 minute and the DNA column was eluted with 100 µl of heated elution buffer (after 1 minute incubation). The DNA, RNA, and protein samples were stored at -80°C.

***Western Blotting***

Protein was lysed via RIPA lysis buffer (25ml of 1M Tris pH 8.0, 2mL of 0.5M EDTA, 5ml of Triton X-100 (1% final), 5ml 10% SDS (0.1% final), 15ml 5M NaCl, total volume was brought up to 500mL with dd$H_2O$) supplemented with 100x ProteCEASE™ protease inhibitor (600 µl/6 cm dish) after cells were washed twice with 1x PBS. After protein extraction, samples were incubated on ice for 10 minutes and spun down at 10,000 RPM for 10 minutes at 4°C, where the supernatant was transferred to a new microcentrifuge tube. Next, a bicinchoninic acid (BCA) assay was used to determine protein concentration for each sample. Normalization for equal protein loading was completed by dilution each sample in RIPA and 6x loading dye. Finally, samples were denatured for 5 minutes at 95°C and 30 µg of protein was loaded into each well of a 10% sodium dodecyl sulfate-polyacrylamide gel and separated by electrophoresis (SDS-PAGE) for 60 minutes at 160V.

Next, protein was transferred to a nitrocellulose membrane for 1 hour at 24V. The membrane was blocked with 5% milk, washed with tris-buffered saline

with 0.05% Tween-20 (TBST), and incubated in the following antibodies diluted in TBST: mouse anti-p53 (Santa Cruz Biotechnology) 1:1000, mouse anti-flag M2 (Sigma) 1:1000, mouse anti-GAPDH (Millipore) 1:10,000. After primary incubation, the membrane was washed three times in TBST and incubated with a secondary antibody (goat anti-rabbit or goat anti-mouse) diluted 1:20,000 for 30 minutes. Bands were visualized on a LiCor© Odyssey machine.

***Quantitative Real-Time Polymerase Chain Reaction (qRT-PCR)***

Cells were grown to 80% confluence before aspirating the media and washing with 1x PBS. Cells were then lysed in 0.5 ml of Tri Reagent LS, collected, and incubated at room temperature for 5 minutes. 100 µl of chloroform was added to the samples and spun down at 14,000 RPM for 10 min at 4°C. The clear aqueous supernatant was transferred to new 1.7 ml microcentrifuge tubes and RNA was precipitated with a 1:1 dilution of isopropanol, once again spun at 14,000 RPM for 10 min at 4°C. Supernatant was removed and the RNA was washed with 500 µl of 70% ethanol at 4°C for 5 minutes at 14,000 RPM. The supernatant was removed and the pellets were re-suspended in 20 µl of $H_2O$, once dried.

5 µl of RNA was incubated with the follow mixture: 10 µl $H_2O$, 4 µl dNTPs (10mM), and 2 µl of oligo dT (50 µM). The mixtures were incubated at 65°C for 5 minutes and the complimentary deoxyribonucleic acid (cDNA) was synthesized by incubating the above mixture with: 10 µl of $H_2O$, 4 µl RT Buffer, and 2 µl of SuperScript reverse transcriptase. The samples were incubated for 45 minutes at

50°C and standardized to 400 ng/µl after concentrations were determined using the NanoDrop© spectrophotometer.

Lastly, 5 µl of cDNA, 10 µl of $H_2O$, 10 µl of Bioline© SYBR Green PCR mix, and 1 µl (10 µM) of both forward and reverse primers was added to each well of a 96-well ABI-FastOpti plate and assayed via the Eppendorf RealPlex ABI-FastOpti Protocol. Forward and reverse primers used for this study are as follows: AL1 (TATTGATGCTGTTGGTCAGCCA/ TAAGGAAGAAAGGAGCAAGCGA), 18S (CCGATAACGAACGAGACTCTGG/ TAGGGTAGGCACACGCTGAGCC), TLR4 (GACCTGTCCCTGAACCCTAT/ CGATGGACTTCTAAACCAGCCA), TPX2 (ACCTTGCCCTACTAAGATT/ ATGTGGCACAGGTTGAGC), and TNC (GTGCAGAACTCTCCTGTCCAAAT/ ATCTTTGCTCCTTGCAGTCTTTG).

## RESULTS

To date, there are no cell-based models that characterize secondary glioblastoma initiation or progression. To create a model to study the expression of genes that are associated with the development of this cancer, human embryonic astrocyte TERT immortalized (hEAT) cells were purchased from ABM Biosciences. Telomerase reverse transcriptase (TERT) activation lengthens the telomeres in DNA strands, allowing cells that would normally undergo apoptosis (after reaching the Hayflick limit) to continue dividing. These cells were either cultured in Prigrow or in a modified Astrocyte media described below. Cells were transduced with lentiviruses that allowed the stable expression of $IDH1^{R132H}$ alone or in combination with $p53^{R273H}$. Because these cells had only previously been altered through their immortalization with hTERT, the effects of $IDH1^{R132H}$ and/or $p53^{R273H}$ should closely reflect those changes during tumor initiation. Other studies which examined these effects in glioblastomas, used cell lines that had already accumulated all of the changes necessary for highly malignant tumor formation.

### *Validation of hEAT cells as a pure astrocyte origin line*

To validate that hEAT cells acquired from ABM were composed purely of progenitor astrocytes, the Hudmon Laboratory at the Indiana University School of Medicine immunostained these cells for markers of different populations of brain-derived cells. First, they determined whether these cells were incompetent for glutamate uptake, which would be consistent with being of progenitor and not mature/differentiated astrocytes. To also determine if these cells could acquire

glutamate uptake, they were transfected with the either Excitatory Amino Acid Transporter 1 (EAAT-1) or Excitatory Amino Acid Transporter 2 (EAAT-2) (Figure 5). Cells were then challenged with [3H] glutamate in the presence or absence of the glutamate uptake blocker TBOA. The inability of these cells to uptake glutamate unless transfected with either EAAT-1 or EAAT-2 is consistent with them not being differentiated. To validate that these cells were of astrocytic origin, hEAT cells were also immunostained with GFAP, Microtubule-associated protein 2 (MAP-2), CD11b (OX-42) and Oligodendrocyte transcription factor (Olig-2) (Figure 6). Cells strongly immunostained for GFAP, an intermediate filament expressed in astrocytes, but showed no immunostaining for MAP-2, OX-42 or Olig-2. The lack of MAP-2 staining indicates that hEAT cell cultures do not contain any neurons. The lack of staining with OX-42 indicates that they do not contain monocytes, macrophages or granulocytes. The lack of Olig-2 staining shows that there is an absence of oligodendrocytes and motor neurons. These results strongly indicate that the hEAT cells purchased from Applied Biological Materials Inc. are a pure population of fetal/progenitor astrocytes.

### *Testing the effects of different media conditions on the growth of hEAT cells*

We next compared the growth of hEAT cells in Prigrow IV, the recommended media by Applied Biological materials (ABM). This was shown in 2012 to foster astrocyte growth (Prabhu et al.). Prigrow IV media was purchased from ABM and supplemented with 10% FBS and Penicillin/Streptomycin. This media allowed robust cell growth in both 2D and 3D conditions. However, due to the exorbitant

cost of this media, we explored alternative media formulations. We initially tested whether hEAT cells would grow in Dulbecco's Modified Eagle Medium (DMEM) High Glucose supplemented with 10% Fetal Calf Serum (FBS) and Penicillin/Streptomycin. hEAT cells were not found to proliferate under these conditions. We therefore examined how hEAT cells would grow in a formulation that has been shown to work well for growing adult rat astrocytes and referred to as Cortical Astrocyte Media (Astro Media). Through consultation with the Hudmon Laboratory at the Indiana University School of Medicine, we developed the Astro media, which consisted of DMEM High Glucose/10% Fetal Calf Serum (not heat inactivated) with Penicillin/Streptomycin, 2mM glutamine, 1mM Sodium Pyruvate, 5ug/ml NAC, 5ug/ml insulin, and 10uM hydrocortisone. hEAT cells grew in Astro media similarly in both 2D and 3D conditions as was observed in Prigrow IV media. Given the dramatically lower costs for making Astro media, hEAT cells were transitioned to grow in Astro media from the Prigrow IV media. This required that the cells be grown for several passages in 50% Astro, 50% Prigrow IV and then transitioned to 100% Astro media.

***Comparison of growth of hEAT cells in 2D and 3D culture systems***

The environment of a cell or tissue dramatically impacts cellular fate. Intrinsic regulators of the microenvironment include transcription factors and cell division factors. Extrinsic factors in the microenvironment include cell-cell interactions, soluble factors, and extracellular matrix (ECM) interactions. The correlation between extrinsic microenvironmental signals and corresponding

changes in gene expression are directly associated with either long-term maintenance or lineage specific differentiation in stem cells (Liu, Lin and Roy).

The ability to study the human brain, and the cells that compose it, is a complex challenge. To mimick the physiological cellular conditions (Preynat-Seauve et al.), a 3-Dimensional culturing environment composed of Corning® Matrigel® Matrix was used. We predicted that progenitor or stem cells might transition to a more differentiated form when switched from a 2-Dimensional to a 3-Dimensional environment containing Matigel® (Liu and Roy). This is inpart because Matrigel® is a solubilized basement membrane preparation extracted from the Engelbreth-Holm-Swarm (EHS) mouse sarcoma, which is rich in ECM proteins like laminin, collagen IV, heparin sulfate proteoglycans, entactin/nidogen, and various growth factors (Liu, Lin and Roy).

hEAT cells were grown on both 2D plastic and 3D Matrigel® cultures for comparison. Genes identified by *Barres et al* are signatures of progenitor or differentiated astrocytes. They were used as indicators of whether hEAT cells grown in 3D showed a transition from a progenitor state to a more differentiated state (Table 2). The sequences for the primers to measure these genes were identified from the Barres publication or in other published articles. The relative levels of APC specific mRNAs and differentiation specific mRNAs were notably decreased in cells grown in 3D (Figure 7). Thus, these cells likely transition away from a progenitor status, but do not seem to be appreciably differentiating. There are a number of reasons for the transition to remain incomplete, likely from inadequate media

conditions. Further experiments need to be conducted with various astrocyte medias that promote differentiation.

### *Stable Heterologous expression of IDH and p53 Mutants in hEAT Cell Lines*

The majority of lower grade astrocytomas (~80%) have mutations in IDH1 and ~65% of these cells also contain a mutation in p53. We determined this overwhelmingly involved an R to H change at residue 132 in IDH and an R to H change at residue 273 in p53 (Ohgaki and Kleihues). Lentiviruses expressing either IDH1 R132H or p53 R273H were therefore constructed. Heat cells were transduced with these lentiviruses in a stepwise fashion and cultured individually to create cells expressing either a control flag, $IDH1^{R132H}$, $p53^{R273H}$ or the combined expression of $IDH1^{R132H}/p53^{R273H}$ (Figure 8). Expression was then validated by immunoblot analysis (Figure 9).

### *Characterization of hEAT cells expressing IDH or p53 mutations in 2D and 3D cultures*

The transduced hEAT cell lines mentioned above were grown to confluence in 10 cm culture dishes, counted on a hemocytometer, and split into either 3.5 cm culture dishes (150,000 cells) with Matrigel© or 6 cm plates (250,000 cells) as a monolayer. They were grown for 5 days (120 Hours) at 37°C. Images were taken every 24 hours and recorded. After 5 days there were no noticeable differences in 2D culturing between the various conditions.

However, after 5 days there were significant changes in the morphology of the cells between the different conditions in 3D (Figure 10). In control cells, the images showed a gradual growth and noticeable interactions between cells. In the $IDH1^{R132H}$ cell line, cells remained small and isolated over the five-day period. The $IDH1^{R132H}$ + $p53^{R273H}$ cell line created a similar but less pronounced lattice structure observed in the control group, although this began to deteriorate after 5 days. In the $p53^{R273H}$ mutant cell line, the cells grew as large clumps.

***Preliminary Data for Next-Generation Sequencing***

In order to conduct the next-generation sequencing analysis, DNA and RNA had to be purified from the hEAT cell lines. This was possible by using the AllPrep® DNA/RNA/Protein kit by Qiagen®. hEAT cell lines had to be scaled up in order to produce enough cells for DNA, RNA, and protein purification. When cells reached approximately 90% confluence in each cell line, they were lysed and homogenized in a buffer, which inactivated DNases, RNases and proteases to ensure intact DNA, RNA, and protein was retrieved. The lysate was then spun through a column with a high-salt buffer that selectively bound genomic DNA. The DNA was washed and eluted, rendering it suitable for analysis. The flow-through from the initial DNA column spin was added to an RNeasy column, where total RNA would bind to the membrane and contaminants were washed away. The RNA was then washed and eluted, making it ready for analysis. Protein was subsequently retrieved from the RNA flow-through and stored at -80°C.

The methylome and the transcriptome of three hEAT cell lines; Flag Control, IDH1$^{R132H}$ and the IDH1$^{R132H}$ + p53$^{R273H}$ was determined by next-generation sequencing through the IU Bloomington genomics core. Initial results from the principal component analysis of transcriptome data showed a clustering of Flag control cells drastically separate from both the IDH1$^{R132H}$ and IDH1$^{R132H}$ + p53$^{R273H}$ cell lines, indicating at a genetic level, there was a difference between control and mutant cell lines (Figure 11). The flag control samples and the IDH1$^{R132H}$ + p53$^{R273H}$ both clustered tightly to their replicates, where as the IDH1$^{R132H}$ had variability on the Y-axis clustering. This was accounted for during the transcriptional pathway analysis. The transcripts which showed significant differences between the different cell line conditions were subjected to INGENUITY® pathway analysis. This revealed that IDH1$^{R132H}$ and IDH1$^{R132H}$ + p53$^{R273H}$ induced 686 and 1830 differentially expressed genes between these two conditions compared to the flag control, respectively. Interestingly, most genes altered by IDH1$^{R132H}$ were similarly impacted in IDH1$^{R132H}$ + p53$^{R273H}$ cell lines (Figure 12). Additionally, diseases, biological functions, and associated networks were identified (Figure 13). This revealed a vast array of results. In the presence of solely the IDH1$^{R132H}$ mutant, astrocytes are associated with cellular movement, growth, proliferation, signaling, and post-translational modifications. They are also engaged in networks relating to cancer, injury, developmental disorders and cell death/survival. They positively regulate genes directing brain development, damage response, proliferation, neuronal survival and inflammatory response, while negatively regulating genes directing differentiation, amino acid and sodium transport, neurogenesis, CNS development,

metabolism, and intermediate filaments. The addition of the $p53^{R273H}$ mutation shares many similar consequences as the $IDH1^{R132H}$ mutation, but has unique characteristics. The double mutant has similar biological functions such as cellular movement, signaling, growth and proliferation, but also shows an association with cellular assembly, organization, function, and maintenance. It also shares networks such as inflammatory disease, cancer, injury and cell death/survival, but associates with networks like movement and immune cell trafficking. Finally, the double mutant has unique upregulated genes involved in tumor initiation and downregulated genes involved in cell polarity. Although the two mutant cell lines share many similarities, there is a clear difference in their genetic makeup and associated networks.

***The YAP-TEAD interaction may be a potential target for molecular inhibition***

The Hippo signaling pathway is identified as one of several pathways known to mediate the majority of cell fate decisions in metazoans (Pan). The HIPPO pathway regulates differential signaling between the inside and outside cells, and when HIPPO is inactivated, hypo-phosphorylated YAP localizes to the nuclei and interacts with transcription factors, including transcriptional enhancer activation domain family members (TEADs) (Zhou et al.). Conversely for the inner cells, HIPPO is activated and YAP is phosphorylated by Lats and sequestered in the cytoplasm (Nishioka et al.). A major player in the Hippo pathway is TEAD4, which is one member of a family of TEA binding domain (TEAD) transcription factors. TEAD is critical for YAP functions in gene expression, cell proliferation, anchorage-

independent growth, and epithelial-mesenchymal transition (Zhou et al.). TEAD4 contributes to the fate of cell lineage specification and its transcript levels have been found to be amplified in a variety of cancers, including testicular, brain, ovarian, head and neck. YAP is a transcriptional co-activator and a potent growth promoter with a TEAD binding domain. YAP overexpression has been shown to increase organ size in *Drosophila* and saturation cell density in NIH3T3 cells (B. Zhao et al.). YAP overexpression and increased nuclear localization in multiple types of human tumors is associated with stem cell properties and cancer metastasis. YAP also cooperates with Myc oncogenes to stimulate tumor growth in nude mice (Chen, Loh and Song).

YAP functions as a transcriptional co-activator since it lacks a DNA binding domain. TEAD mediates Hippo signaling in organ size control by functioning as a YAP partner. TEAD transcriptional factors interact with the N-terminal of YAP via their C-terminals. In the structure of the mouse TEAD-YAP complex, TEAD adopts an immunoglobulin-like beta-sandwich fold flanked by four short alpha helices, while YAP resembles a belt wrapped around TEAD via folding into two alpha helices linked by a PXXϕP motif-containing loop (Chen, Loh and Song). The C-terminus of TEAD presents a rigid interface for specific interaction with YAP, while nuclear magnetic resonance (NMR) studies have revealed that the N-terminal TEAD binding domain of YAP exists in an unfolded conformation in its native state and that TEAD binding causes localized conformational changes in YAP (Tian et al.). Only a small fragment in the N-terminal region of YAP is involved with the interaction of TEAD. In this fragment are three important binding regions identified by *Chen et al 2010*,

which include two alpha helices and the PXXϕP motif containing linker region, which are required for interaction between YAP and TEAD and are crucial specificity determinants.

Multiple TEAD constructs were created as potential screening targets for inhibiting the YAP-TEAD interaction. One construct was TEAD1 with an 80 base pair manipulation. The original full length TEAD1 construct (Figure 14) contained a common ATG start site. However, this was an incorrect start site for the fragment, which required an ATT sequence at the start site. A front-end gBlock® gene fragment was synthesized, ordered, and received from Addgene. It was constructed in the pUC57 vector (Figure 15). From there, it was digested out of pUC57 with restriction enzymes Asc1 and Mfe1 and ligated into the p-GEX-6p-1 plasmid, which contained a truncated version of TEAD1 also cut with Asc1 and Mfe1 to remove the improper front end. This newly synthesized fragment contains the proper ATT start site for TEAD1 instead of the more common ATG start site. Another construct created was a smaller, manipulated version of TEAD4 (Figure 16) that was PCR amplified out of a different p-GEX-6p-1 plasmid. It was cloned into the His-tagged Pet28a (+) vector with restriction enzymes HindIII and BamHI. Both completed constructs were handed to the Georgiadis Laboratory at the Indiana University School of Medicine to be tested for expression and sent off to screen for small molecule inhibitors of the YAP-TEAD interaction.

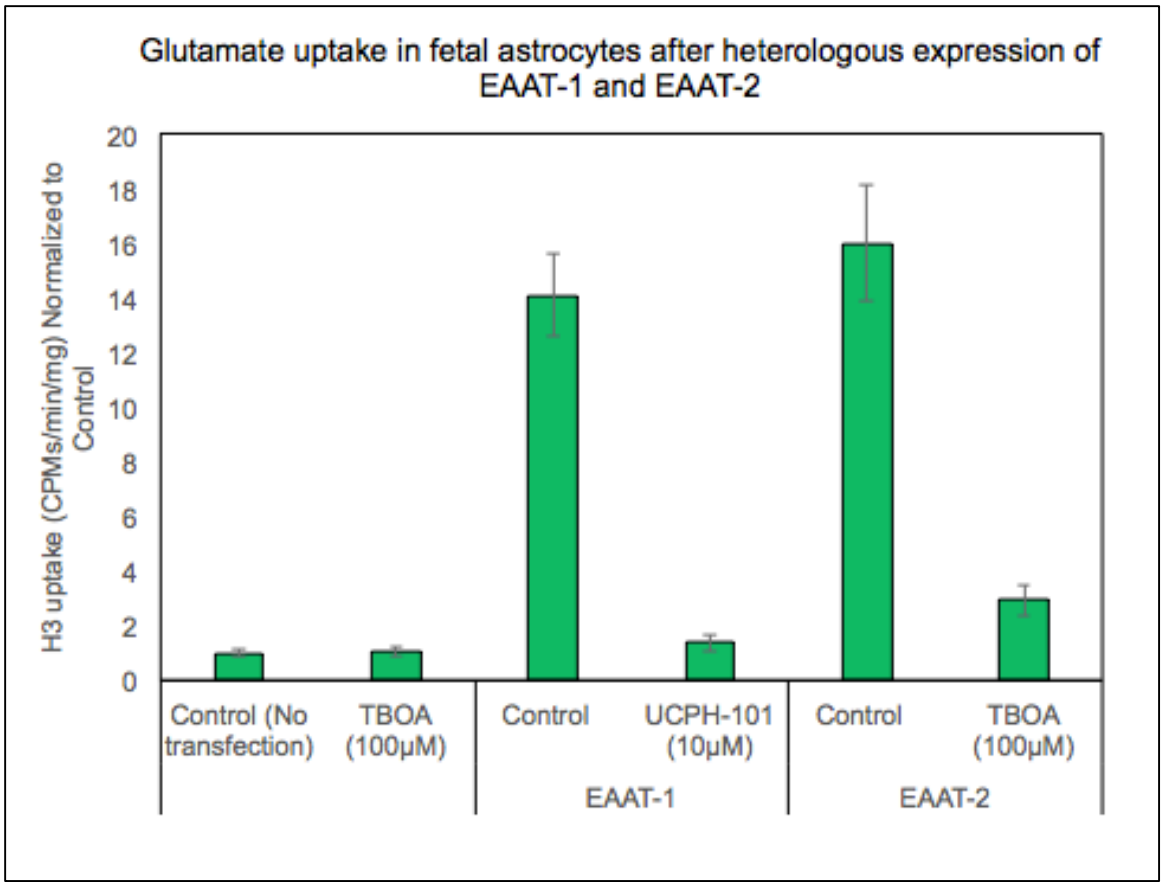


Figure 5. **Glutamate Uptake in Fetal Astrocytes After Heterologous Expression of EAAT-1 and EAAT-2.** Naïve hEAT cells do not take up glutamate but are capable of gaining sensitivity to glutamate uptake following heterologous expression of either EAAT-1 or EAAT-2. Cells were also challenged with glutamate uptake in the presence of glutamate uptake inhibitors TBOA and UCPH-101. (Experiment carried out by the laboratory of A. Hudmon at IUSM)

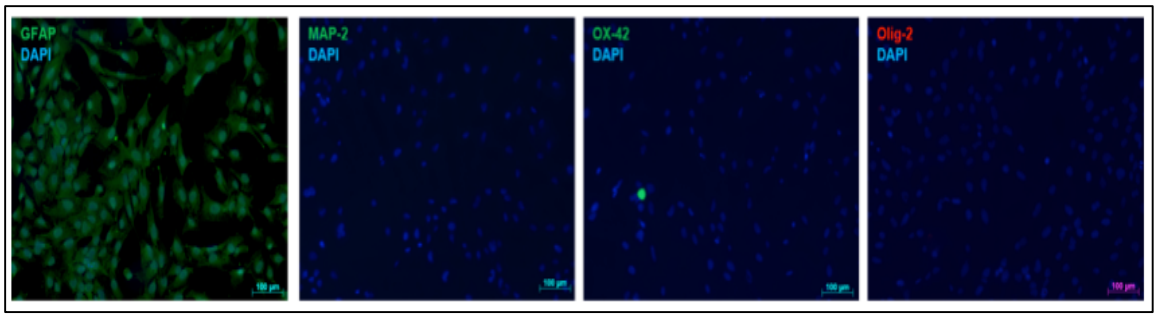


Figure 6. **Fetal Astrocytes are GFAP Positive, but Negative for MAP-2, OX-42 and Olig-2.** hEAT cells were cultured on glass coverslips before being fixed, permeabilized, and immunostained for GFAP (astrocyte marker), MAP-2 (neuron marker), OX-42 (macrophage marker), Olig-2 (oligodendrocyte marker) and DAPI (nuclear and chromosome marker). (Experiment carried out by the laboratory of A. Hudmon at IUSM)

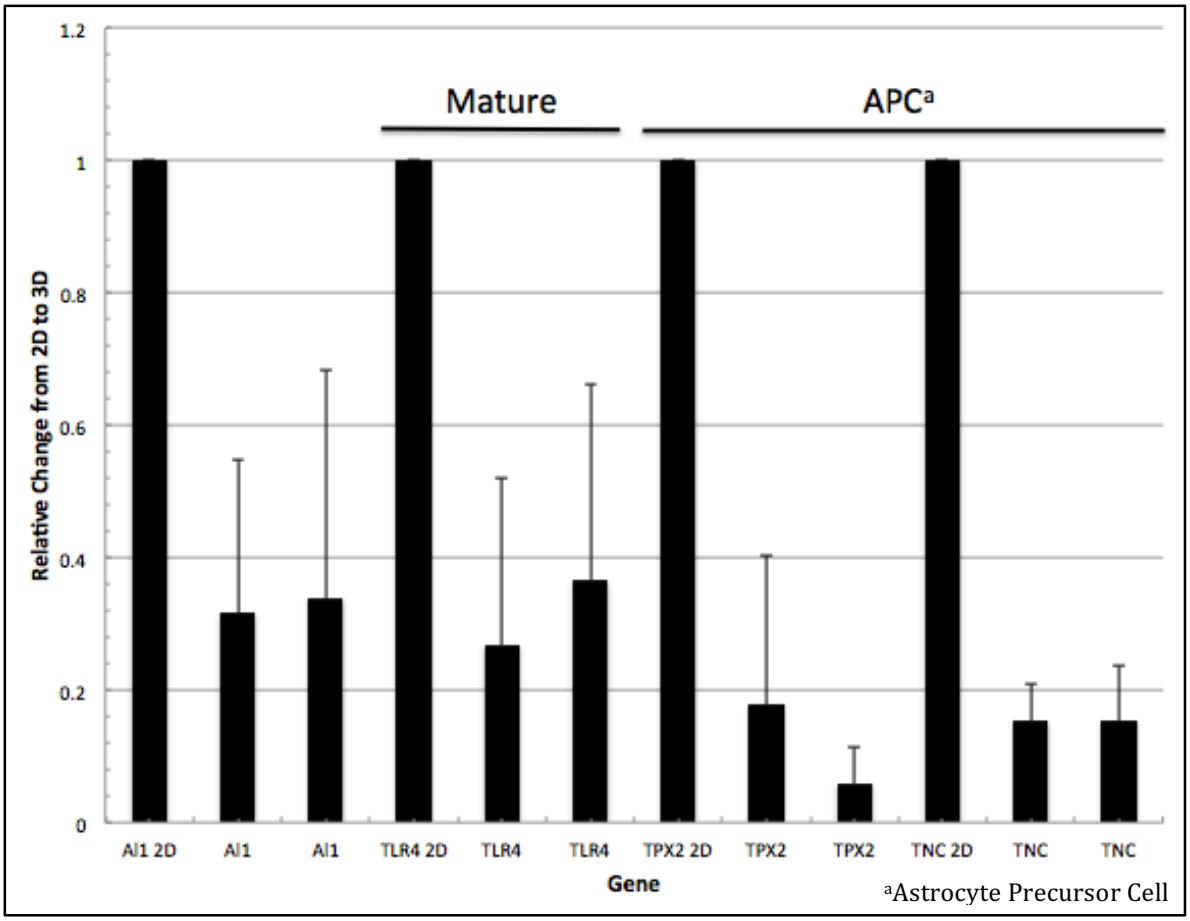


Figure 7. **Relative Change in the Levels of mRNA Signatures of Progenitor and Differentiated Astrocytes in hEAT Cells Grown in 2D or 3D Environments.** Cells were cultured on plastic or in Matrigel© for 4 days before being recovered and lysed in TRIzol® to isolate total mRNA. cDNA was then produced using reverse transcription. The relative levels of the indicated genes were measured by qRT-PCR. Measurements were conducted in biological triplicate and technical duplicate. Overall, both adult differentiation markers and APC markers were found to be reduced in hEAT cells grown in 3D vs 2D cultures.

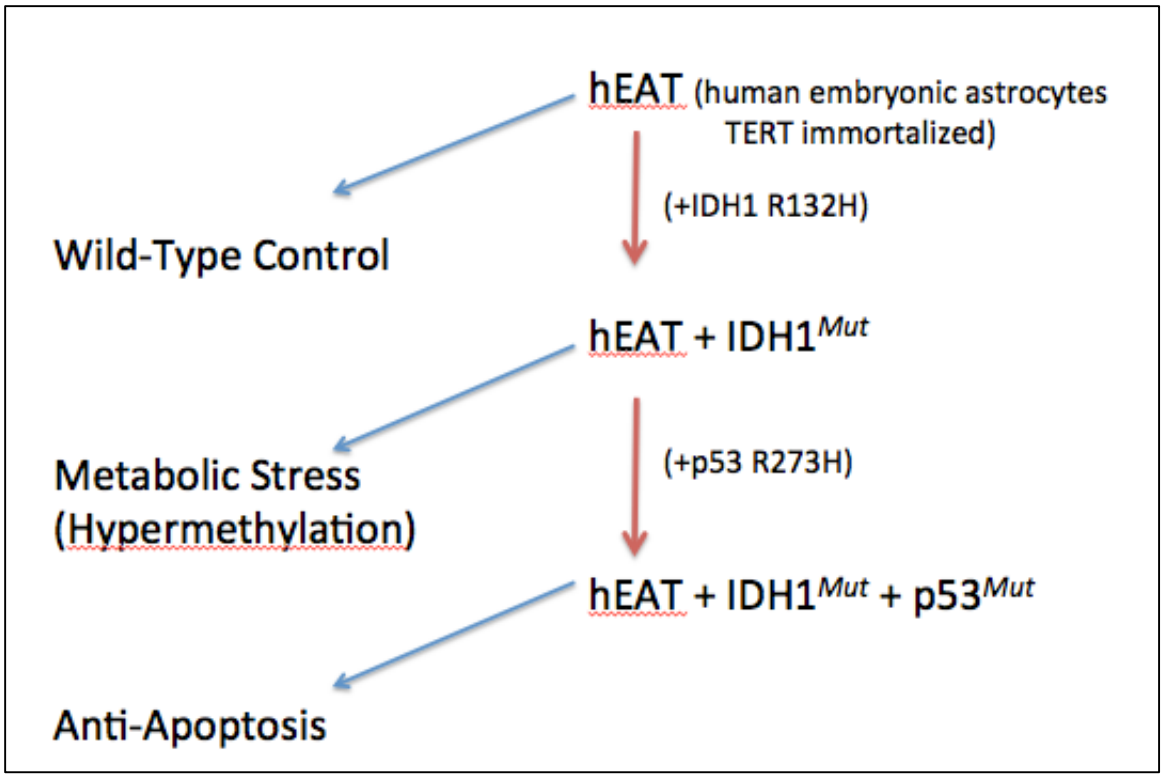


Figure 8. **The Proposed Model for the Secondary Glioma Initiation Series.** The overall workflow whereby hEAT cells were transduced with a lentivirus expressing $IDH1^{mut}$ or $IDH1^{mut}$ + $p53^{mut}$. Control hEAT cells were infected with a control mCherry tag, mCherry tagged-$IDH1^{R132H}$ or with both $IDH1^{R132H}$ + $p53^{R273H}$ viruses. The predicted cellular properties from the expression of these proteins is also indicated on the left.

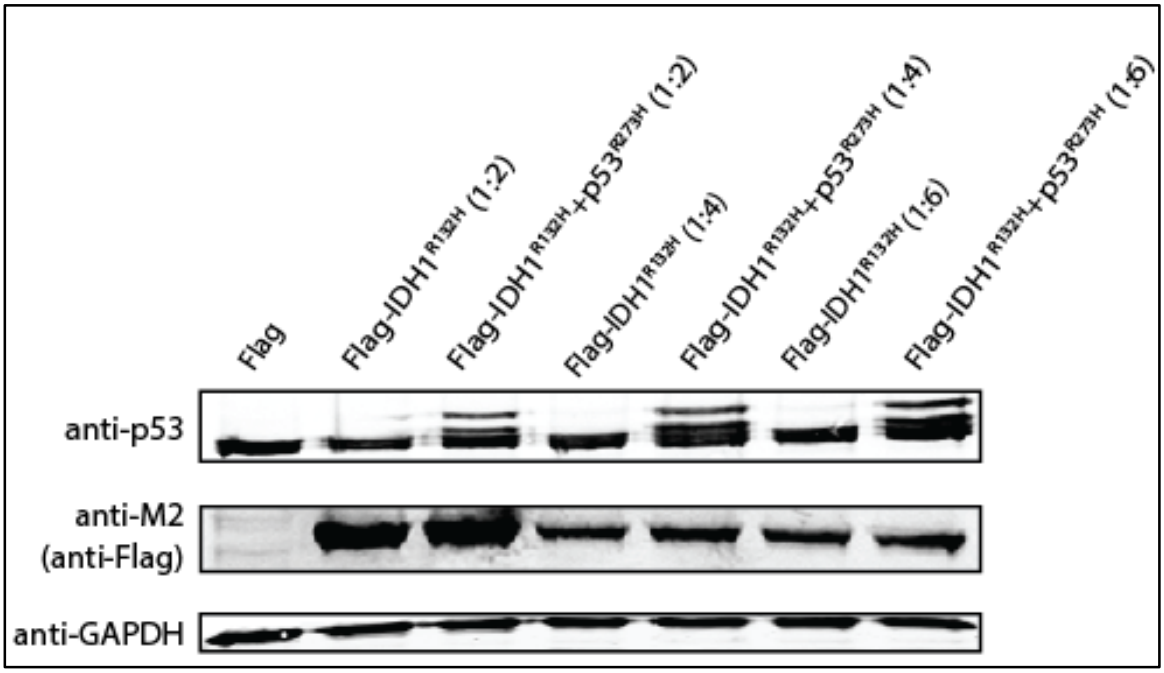


Figure 9. **Western Blot Validating Overexpression of IDH1$^{R132H}$ and p53$^{R273H}$.** Cell lines transduced at the indicated dilutions with lentiviruses expressing the indicated proteins were grown in appropriate media until approximately 80% confluent. Then lysed and analyzed by western blot. The viral media was diluted with complete DMEM, as indicated in (X:X) to help with toxicity.

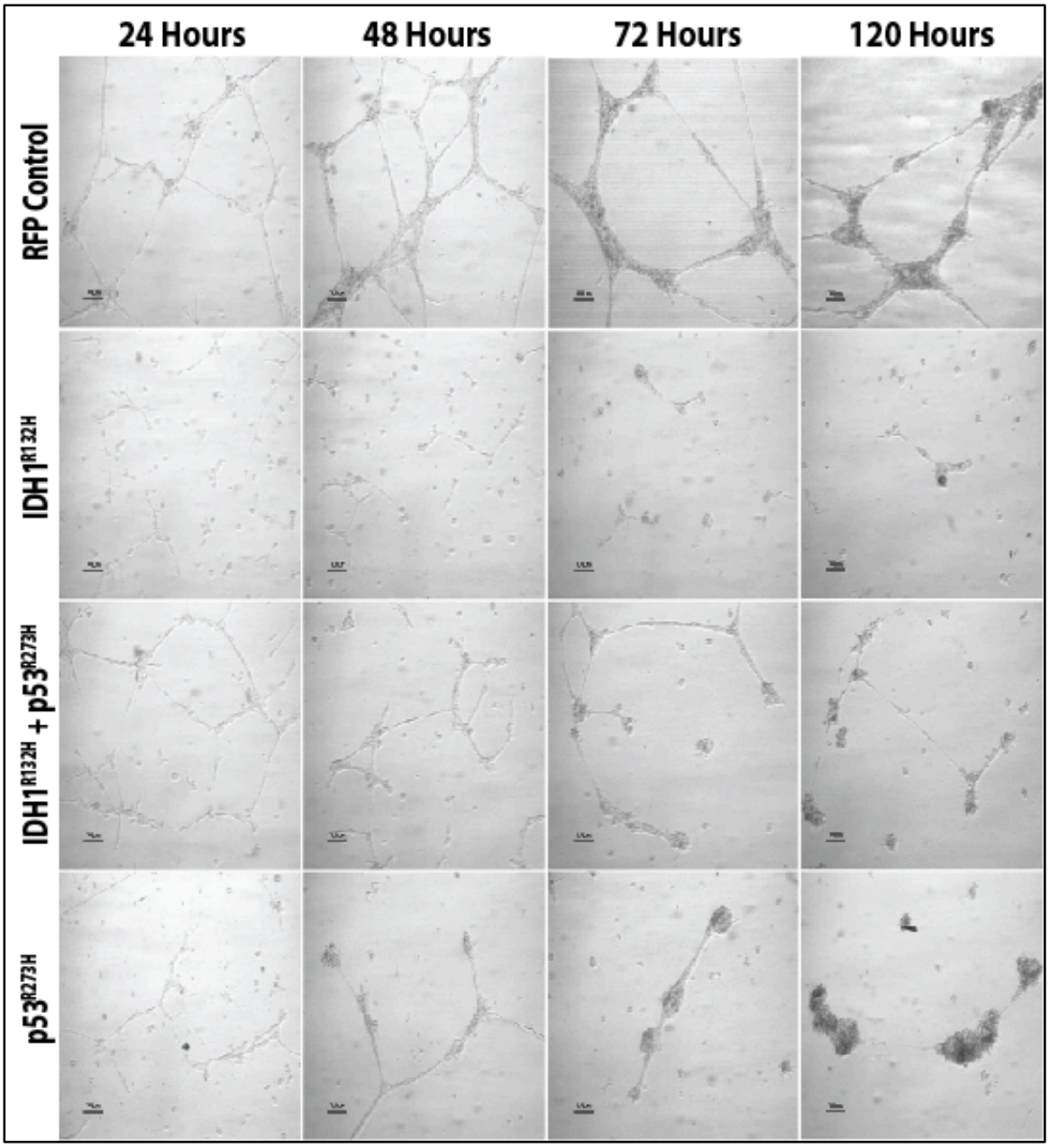


Figure 10**. Secondary Glioma Initiation Series Plated in 3D Matrigel.** When cultured on a 3-Dimensional environment (Matrigel®), hEAT cell lines showed specific phenotypes depending on the expression of Control, $IDH1^{R132H}$, $p53^{R273H}$ or $IDH1^{R132H}$ + $p53^{R273H}$ over a 5-day period. The control hEAT cells formed large cells that strongly connected to neighboring cells. Expression of $IDH1^{R132H}$ alone resulted in cells that failed to increase in size or form connections with neighboring cells. Expression of $p53^{R273H}$ resulted in a moderate reduction in intercellular connectivity initially, but a collapse of these connections by Day 5. Expression of both IDH1 and p53 mutations resulted in cells that partially rescued the control phenotype, where cells were larger and more interconnected versus cells expressing $IDH1^{R132H}$ alone.

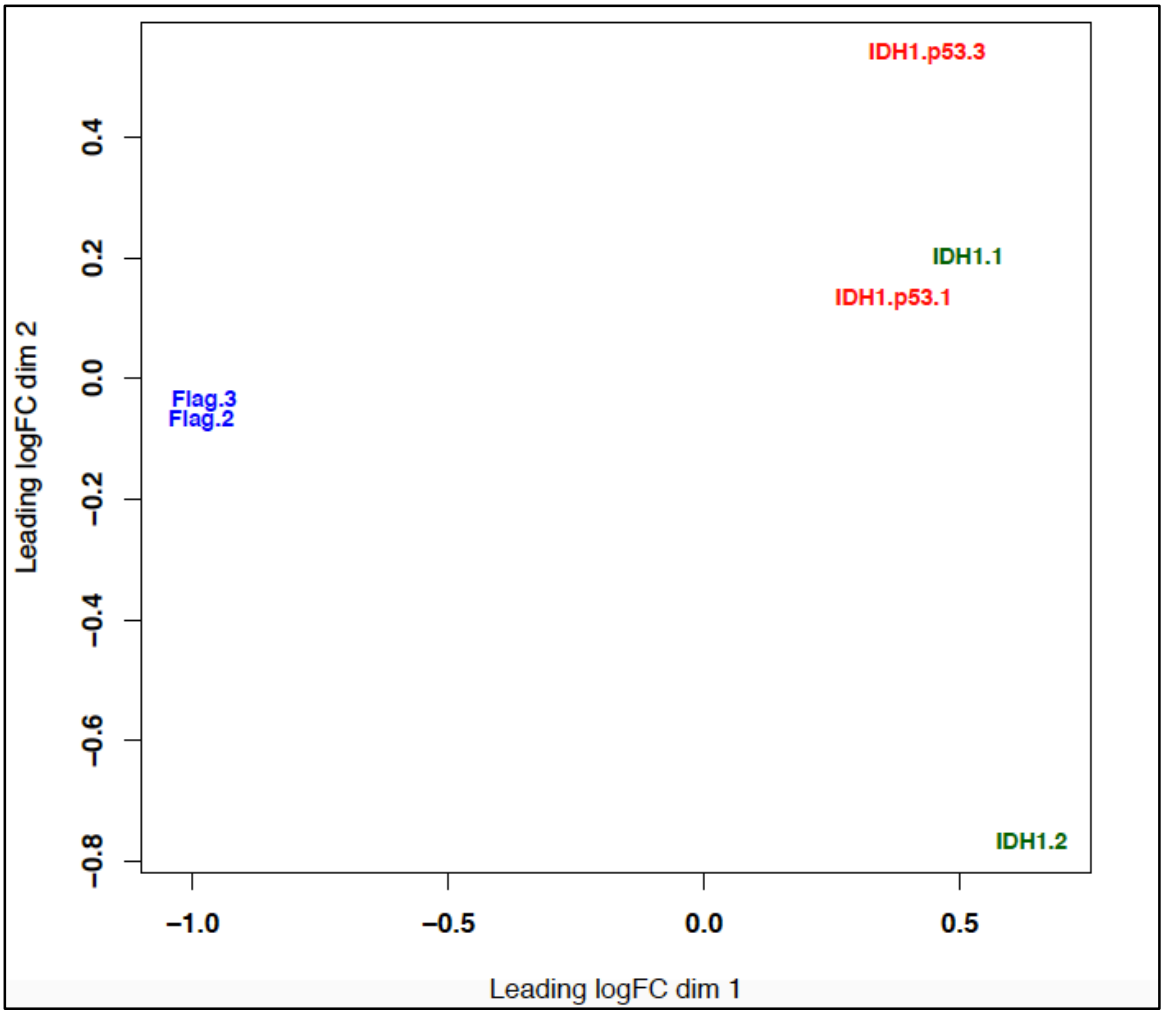


Figure 11. **Next-Generation Sequencing Results Reveal Significant Difference Between Flag Control hEAT Cells Versus Mutated hEAT Cell Lines.** A principal component analysis from the next-generation sequencing transcriptome analysis showed a clustering of Flag control cells drastically separate from both the $IDH1^{R132H}$ and $IDH1^{R132H}$ + $p53^{R273H}$ cell lines.

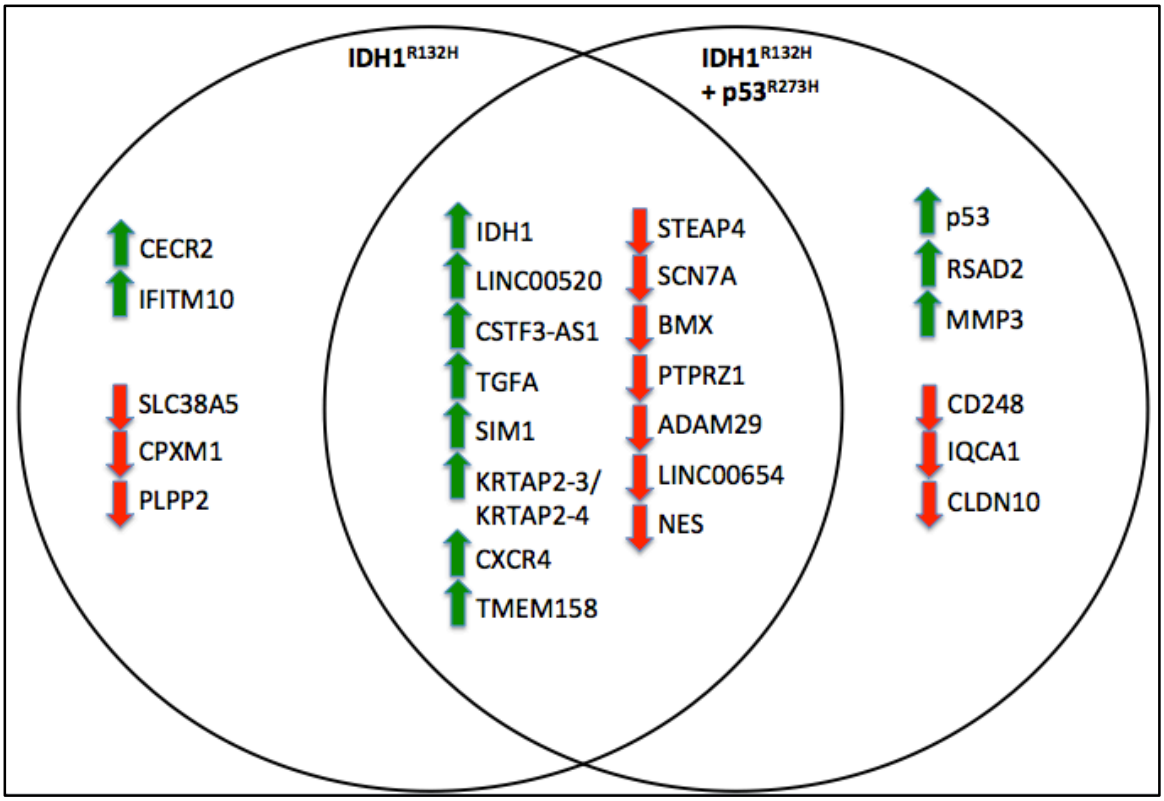


Figure 12. **A Venn Diagram Showing Shared and Unique Genes in the IDH1 and IDH1+p53 Mutant Cell Lines.** The use of next-generation sequencing and transcriptome analysis revealed unique genetic signatures between the $IDH1^{R132H}$ and $IDH1^{R132H}$ + $p53^{R273H}$ cell lines. The majority of genes were similar in their regulation; however, both mutants showed a unique set of genes being up and downregulated. In total, $IDH1^{R132H}$ had 686 differentially expressed genes and $IDH1^{R132H}$ + $p53^{R273H}$ had 1830 differentially expressed genes.

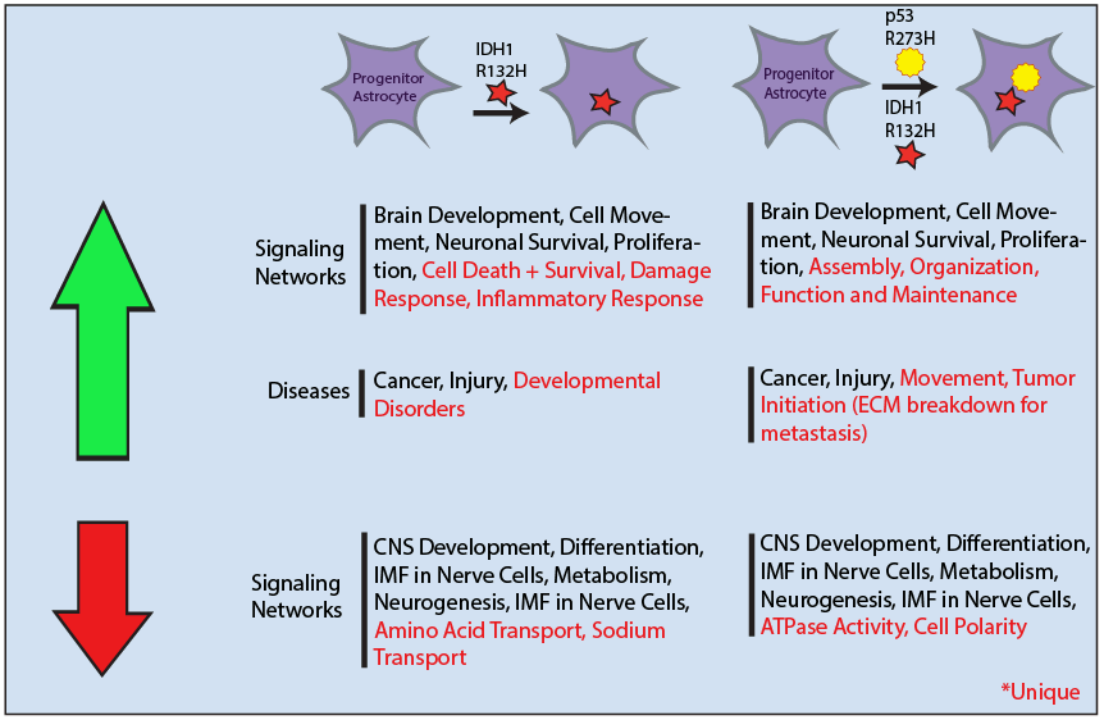


Figure 13. **The Cellular Consequences of Genetic Mutations in Astrocytes.** Transcriptome analysis revealed unique functions and networks associated with mutant cells lines relative to the control astrocytes. Both mutants had similarities and differences in their results. Results highlighted in red are unique to the cell lines they are associated with.

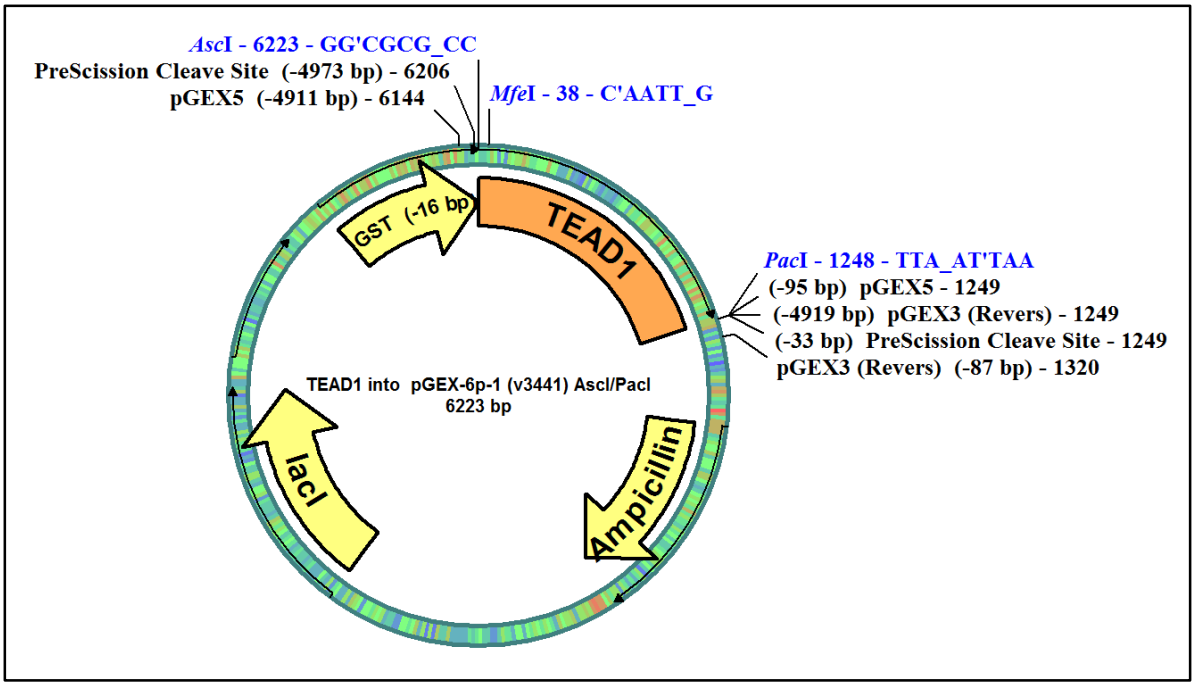


Figure 14. **Restriction Map of TEAD1 in pGEX-6p-1.** The TEAD1:pGEX-6p-1 plasmid construct contains restriction enzyme cut sites at base pair locations 38 and 6223. These sites were digested to truncate the front end of TEAD1 to allow remodeling.

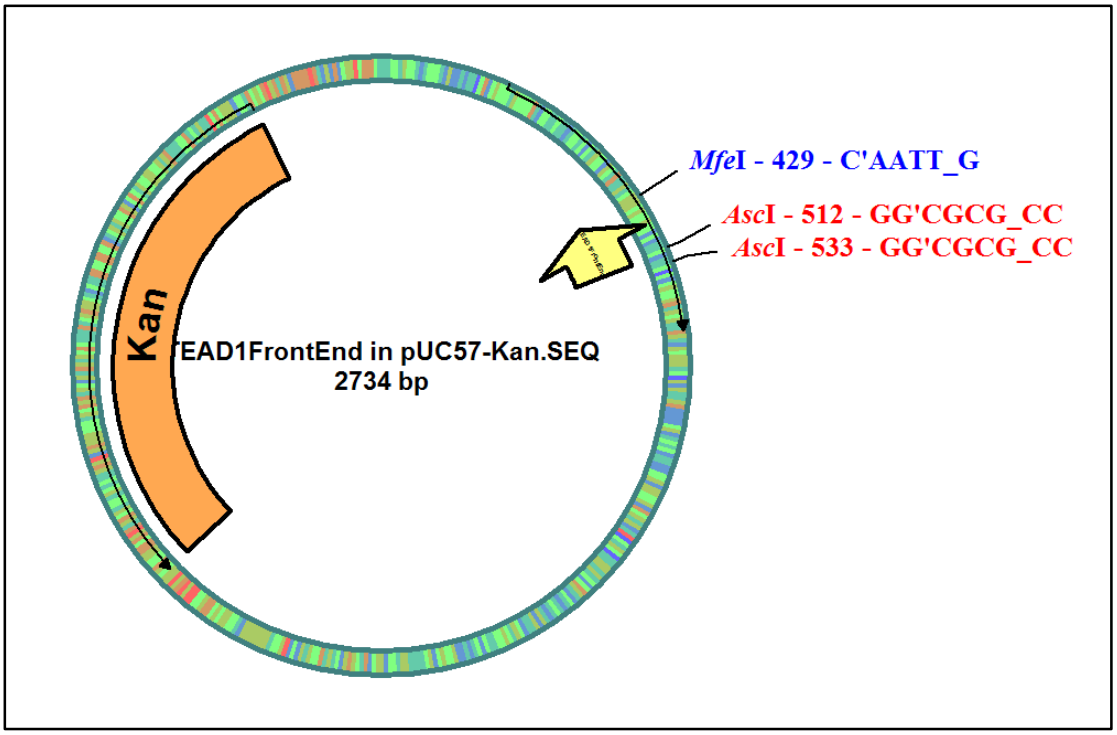


Figure 15. **Restriction Map of TEAD1 Front End Piece in pUC57 Vector.** The TEAD1FrontEnd piece was created with restriction enzyme locations at 429 and 512. These sites were cleaved with MfeI and AscI enzymes to remove the piece from the pUC57 plasmid in order to complete the TEAD1 construct in the pGEX-6p-1 vector.

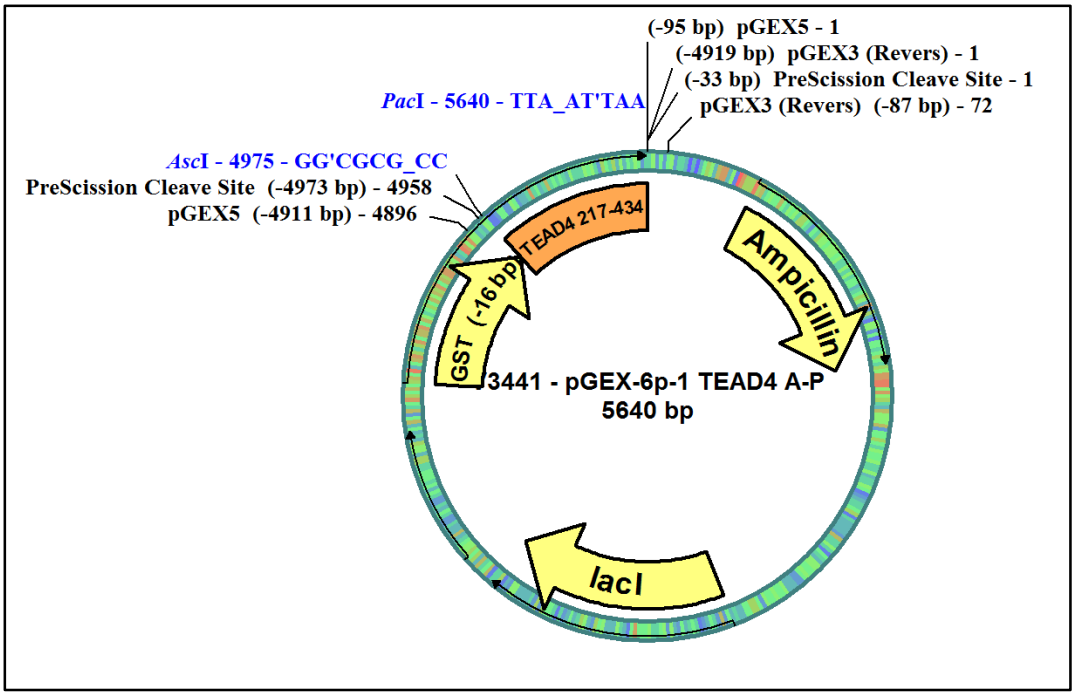


Figure 16. **Restriction Map of TEAD4 Insert in pGEX-6p-1.** A smaller, manipulated version of TEAD4 was inserted into the pGEX-6p-1 plasmid via restriction enzymes AscI and PacI at base pair locations 4975 and 5640, respectively.

## DISCUSSION

### *Creating and Characterizing Secondary Glioblastoma in Cell Lines*

Our current model of secondary glioblastomas indicates that the presence of $IDH1^{R132H}$ blocks differentiation of astrocytes (Figure 17). This mutation is then compounded with additional mutations in p53 or ATRX, which add resistance to the cellular stress being induced by IDH1 mutations and thereby confer survival advantages to these cells. It is proposed that over time, these cells transform into lower grade gliomas. The 7-10 year indolent phase we propose is exited as cells progressively lose AmotL1 and/or AmotL2, which subsequently contributes to invasiveness and high malignancy.

To model how $IDH1^{R132H}$ and $p53^{R273H}$ impact normal progenitor astrocytes, we developed a series of cell lines in which these mutations were introduced. We further tested how growing these cells in a 3D culturing environment might promote a loss of progenitor status and a proclivity to acquire characteristics of differentiated astrocytes (Liu, Lin and Roy). This seems to be occurring based on the morphology of these cells after several days of culturing in 3D Matrigel®. RFP control cells formed intercellular contacts that likely involve communication and signaling, which is known to occur between astrocytes in an *in vivo* setting. This is known to correlate with an overall increase in cell survival, communication, and growth. However, cells expressing only $IDH1^{R132H}$ looked to initially make connections, but this rapidly deteriorated by 48 hours. The $IDH1^{R132H}$ + $p53^{R273H}$ expressing cells were seen to thrive better than cells expressing $IDH1^{R132H}$ alone, although not to the same extent as the control cells. Further, they showed some

capacity to connect with neighboring cells. It's suggested that the addition of the $p53^{R273H}$ dominant-negative mutation is reducing the apoptotic response in the cells. Accordingly, there was a large difference in growth between the $IDH1^{R132H}$ + $p53^{R273H}$ mutants compared to the $IDH1^{R132H}$ mutant alone. These results support the theory that the mutated form of IDH1 blocks differentiation in otherwise normal astrocytes and increases cellular stress. Further, the addition of a specific mutation in p53 helps allow the mutated cells to survive in the presence of mutant IDH1 stress. This is the basis of secondary glioblastoma, and future experiments will be conducted adding AmotL1 and/or AmotL2 mutations to follow progression.

We also characterized the molecular changes in these cell lines through the use of next-generation sequencing experiments that measured transcriptome and methylome data. Cytosine methylation can significantly affect both gene expression and chromatin remodeling. It regulates spatial and temporal gene expression and is critical for embryonic development and differentiation processes. Cytosine methylation in promoter regions often reduces gene expression; where as heterochromatin (inactive chromatin) formation is driven by hypermethylation. Accordingly, 88% of active promoters are unmethylated in mammals. However, if abnormal hypomethylation in heterochromatin occurs, there is an increased risk of chromosomal instability and loss of genomic imprinting (Illumina). Importantly, methylation can help drive differentiation in cells, where they typically don't revert back to stem cells. By determining which genes are being hyper- or hypo-methylated, it's possible to identify a progression of mutations in secondary glioblastomas.

Additionally, transcriptome analysis can characterize all coding and non-coding transcriptional activity. This can focus on a subset of relevant target genes and transcripts, or profile thousands of genes simultaneously to create a whole picture of cellular function (Illumina). This provides an overview of actively expressed genes and transcripts under mutated conditions.

Based on the results from the next-generation transcriptome analysis, there appears to be a transition from a progenitor cell to a more invasive, stem-like cell. Transcriptome analysis revealed a significant clustering difference between the control hEAT cell line and the mutant hEAT cell lines. This indicates there are clear molecular changes occurring between the cell lines in the series. Although not definite, there are indications that this transition is taking place across the three cell lines by genetic regulation. Both the $IDH1^{R132H}$ and the $IDH1^{R132H}$ + $p53^{R273H}$ cell lines show an association with biological functions including cell movement, growth, proliferation and signaling. However, unique to the $IDH1^{R132H}$ + $p53^{R273H}$ is the association with cellular assembly, organization, function and maintenance. Indicating, the addition of the $p53^{R273H}$ mutation may create a stress resistance, allowing cells to regain functional abilities. There are a number of genes being up and downregulated similarly between the two mutant cell lines, but each line contains a few unique regulations. In the $IDH1^{R132H}$ cells, CECR2 and IFITM10 are being upregulated, while SLC38A5, CPXM1, and PLPP2 are being downregulated. Conversely, RSAD2 and MMP3 are upregulated in $IDH1^{R132H}$ + $p53^{R273H}$, whereas CD248, IQCA1, and CLDN10 are being downregulated. Each gene is unique in function, but perhaps the most interesting is the upregulation of MMP3 in the

IDH1$^{R132H}$ + p53$^{R273H}$ cell line. MMP3 (Matrix Metallopeptidase 3) is a key enzyme required for extracellular matrix breakdown, and heavily involved in cellular development, tissue remodeling and metastasis, with direct association to glioma progression. Further, CLDN10 (Claudin 10) is an enzyme heavily involved in maintaining cell polarity. CLDN10 is downregulated in the IDH1$^{R132H}$ + p53$^{R273H}$ cells, supporting the claim that these cells are losing polarity as they transition to an invasive phenotype. The platform for repeating this series is set for future studies, where the cell lines will be replicated and sequenced for a full analysis of RNA transcriptome and DNA methylome sequencing. Importantly, the drastic phenotypic differences in 3D culturing, as well as clustering from next-generation sequencing data are strong indications that these mutations are causing the predicted genetic and molecular changes.

### *Targeting the YAP-TEAD Interaction for Drug Development*

There is an unmet need to find new drugs in cancer development that target selectively in signaling pathways for cancer cell growth, while having minimal effects on normal tissues. The Hippo pathway has been continuously demonstrated as an important pathway for growth control and tissue regeneration in organisms ranging from *Drosophila* to humans and may be the key to finding pathways that can be manipulated for successful molecular development (Zhou et al.).

It has been shown that the loss of TEAD has little consequence on normal liver growth while suppressing tumorigensis driven by YAP overexpression (Zhou et al.). Targeting the YAP binding surface on TEAD, by both designing a peptide

molecule that mimics the region of YAP bound to TEAD in the structure and/or a small molecule that selectively blocks any of the three important binding regions between YAP and TEAD, might be an effective strategy to abolish the YAP-TEAD interaction and may have anticancer potential (Chen, Loh and Song).

So far, multiple compounds have been created for use in YAP-TEAD screenings. Collectively, derivatives of TEAD1, TEAD2, and TEAD4 are either complete or in the process of being constructed for these screens. Future results from these compounds will likely lead to inhibitory compounds that are specific to the YAP-TEAD interaction. By having the ability to inhibit the YAP-TEAD interaction, YAP dependent transcription can be controlled, potentially halting tumor progression.

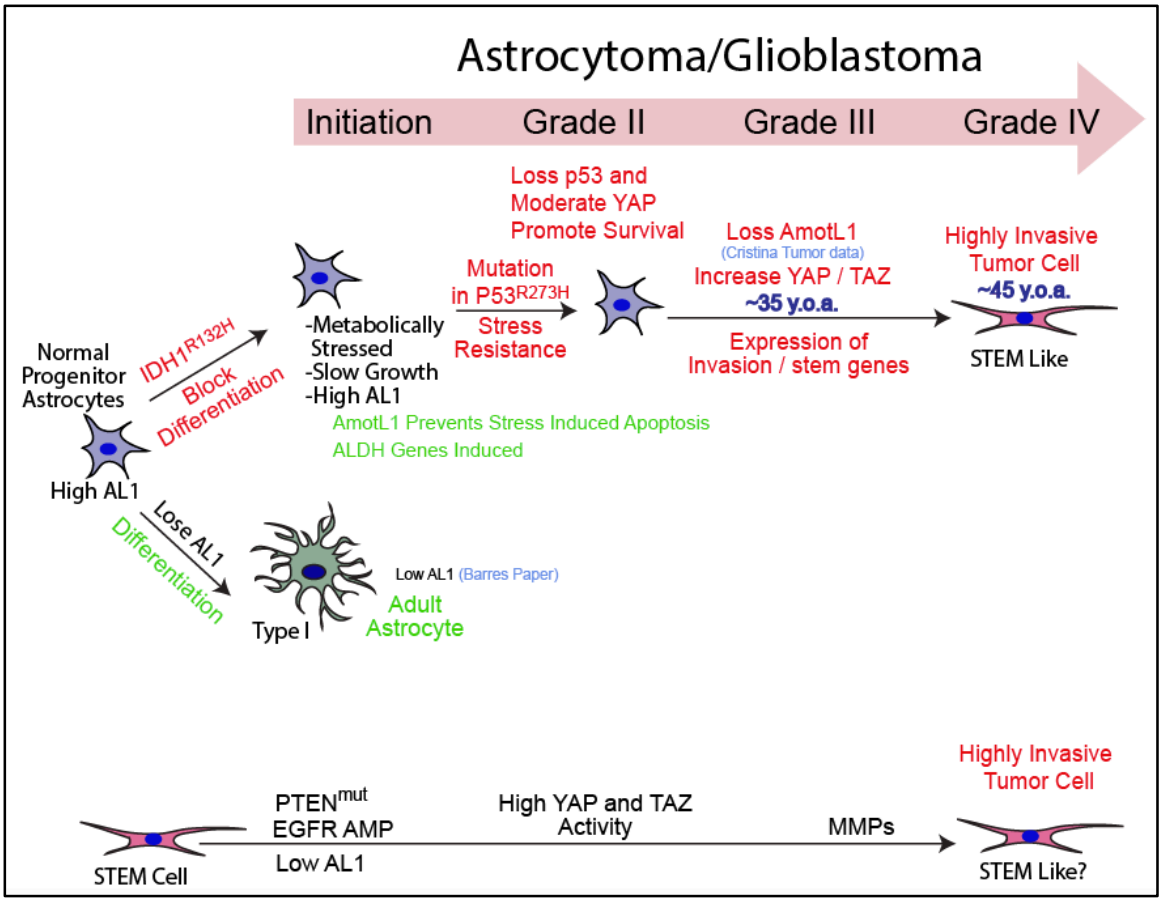


Figure 17. **Conceptual Model of Secondary Glioblastoma Initiation and Progression.** Progenitor astrocytes normally differentiate unless they experience mutations that drive them to become tumorigenic. Normal, healthy astrocytes will lose AL1 levels as they undergo differentiation in order to become an adult astrocyte. However, if the IDH1$^{R132H}$ mutation is acquired, that differentiation pathway is blocked, and the metabolically stressed astrocytes retain high AL1 levels. Data from the TCGA indicates that as these cells become more malignant, they concomitantly lose AmotL1 expression.

## REFERENCES


Adler, J. J., et al. "Amot130 Adapts Atrophin-1 Interacting Protein 4 to Inhibit Yes-Associated Protein Signaling and Cell Growth." *J Biol Chem* 288.21 (2013): 15181-93. Print.

Agnihotri, S., K. D. Aldape, and G. Zadeh. "Isocitrate Dehydrogenase Status and Molecular Subclasses of Glioma and Glioblastoma." *Neurosurg Focus* 37.6 (2014): E13. Print.

Aldape, K., et al. "Glioblastoma: Pathology, Molecular Mechanisms and Markers." *Acta Neuropathol* 129.6 (2015): 829-48. Print.

Bao, S., et al. "Glioma Stem Cells Promote Radioresistance by Preferential Activation of the DNA Damage Response." *Nature* 444.7120 (2006): 756-60. Print.

Chen, L., P. G. Loh, and H. Song. "Structural and Functional Insights into the Tead-Yap Complex in the Hippo Signaling Pathway." *Protein Cell* 1.12 (2010): 1073-83. Print.

Ferris, S. P., et al. "Idh1 Mutation Can Be Present in Diffuse Astrocytomas and Giant Cell Glioblastomas of Young Children under 10 Years of Age." *Acta Neuropathol* (2016). Print.

Hanahan, D., and R. A. Weinberg. "The Hallmarks of Cancer." *Cell* 100.1 (2000): 57-70. Print.

Hao, Y., et al. "Tumor Suppressor Lats1 Is a Negative Regulator of Oncogene Yap." *J Biol Chem* 283.9 (2008): 5496-509. Print.

Hegi, M. E., et al. "Mgmt Gene Silencing and Benefit from Temozolomide in Glioblastoma." *N Engl J Med* 352.10 (2005): 997-1003. Print.

Illumina, Inc. "Comprehensive Exploration of the Methylome." 2016. Web.

Jiao, Y., et al. "Frequent Atrx, Cic, Fubp1 and Idh1 Mutations Refine the Classification of Malignant Gliomas." *Oncotarget* 3.7 (2012): 709-22. Print.

Liu, H., J. Lin, and K. Roy. "Effect of 3d Scaffold and Dynamic Culture Condition on the Global Gene Expression Profile of Mouse Embryonic Stem Cells." *Biomaterials* 27.36 (2006): 5978-89. Print.

Liu, H., and K. Roy. "Biomimetic Three-Dimensional Cultures Significantly Increase Hematopoietic Differentiation Efficacy of Embryonic Stem Cells." *Tissue Eng* 11.1-2 (2005): 319-30. Print.

Louis, D. N., et al. "The 2007 Who Classification of Tumours of the Central Nervous System." *Acta Neuropathol* 114.2 (2007): 97-109. Print.

Lu, C., et al. "Idh Mutation Impairs Histone Demethylation and Results in a Block to Cell Differentiation." *Nature* 483.7390 (2012): 474-8. Print.

Nishioka, N., et al. "The Hippo Signaling Pathway Components Lats and Yap Pattern Tead4 Activity to Distinguish Mouse Trophectoderm from Inner Cell Mass." *Dev Cell* 16.3 (2009): 398-410. Print.

Ohgaki, H., and P. Kleihues. "The Definition of Primary and Secondary Glioblastoma." *Clin Cancer Res* 19.4 (2013): 764-72. Print.

Pan, D. "Hippo Signaling in Organ Size Control." *Genes Dev* 21.8 (2007): 886-97. Print.

Parsons, D. W., et al. "An Integrated Genomic Analysis of Human Glioblastoma Multiforme." *Science* 321.5897 (2008): 1807-12. Print.
Prabhu, A., et al. "Targeting the Unfolded Protein Response in Glioblastoma Cells with the Fusion Protein Egf-Suba." *PLoS One* 7.12 (2012): e52265. Print.
Preynat-Seauve, O., et al. "Development of Human Nervous Tissue Upon Differentiation of Embryonic Stem Cells in Three-Dimensional Culture." *Stem Cells* 27.3 (2009): 509-20. Print.
Stupp, R., et al. "Radiotherapy Plus Concomitant and Adjuvant Temozolomide for Glioblastoma." *N Engl J Med* 352.10 (2005): 987-96. Print.
Suva, M. L., et al. "Reconstructing and Reprogramming the Tumor-Propagating Potential of Glioblastoma Stem-Like Cells." *Cell* 157.3 (2014): 580-94. Print.
Suva, M. L., N. Riggi, and B. E. Bernstein. "Epigenetic Reprogramming in Cancer." *Science* 339.6127 (2013): 1567-70. Print.
Tian, W., et al. "Structural and Functional Analysis of the Yap-Binding Domain of Human Tead2." *Proc Natl Acad Sci U S A* 107.16 (2010): 7293-8. Print.
Turcan, S., et al. "Idh1 Mutation Is Sufficient to Establish the Glioma Hypermethylator Phenotype." *Nature* 483.7390 (2012): 479-83. Print.
Waitkus, M. S., B. H. Diplas, and H. Yan. "Isocitrate Dehydrogenase Mutations in Gliomas." *Neuro Oncol* 18.1 (2016): 16-26. Print.
Watanabe, T., et al. "Idh1 Mutations Are Early Events in the Development of Astrocytomas and Oligodendrogliomas." *Am J Pathol* 174.4 (2009): 1149-53. Print.
Weller, M., et al. "Molecular Predictors of Progression-Free and Overall Survival in Patients with Newly Diagnosed Glioblastoma: A Prospective Translational Study of the German Glioma Network." *J Clin Oncol* 27.34 (2009): 5743-50. Print.
Wells, C. D., et al. "A Rich1/Amot Complex Regulates the Cdc42 Gtpase and Apical-Polarity Proteins in Epithelial Cells." *Cell* 125.3 (2006): 535-48. Print.
Wise, D. R., et al. "Hypoxia Promotes Isocitrate Dehydrogenase-Dependent Carboxylation of Alpha-Ketoglutarate to Citrate to Support Cell Growth and Viability." *Proc Natl Acad Sci U S A* 108.49 (2011): 19611-6. Print.
Yan, H., et al. "Idh1 and Idh2 Mutations in Gliomas." *N Engl J Med* 360.8 (2009): 765-73. Print.
Zhang, Y., et al. "Purification and Characterization of Progenitor and Mature Human Astrocytes Reveals Transcriptional and Functional Differences with Mouse." *Neuron* 89.1 (2016): 37-53. Print.
Zhao, B., et al. "Inactivation of Yap Oncoprotein by the Hippo Pathway Is Involved in Cell Contact Inhibition and Tissue Growth Control." *Genes Dev* 21.21 (2007): 2747-61. Print.
Zhao, S., et al. "Glioma-Derived Mutations in Idh1 Dominantly Inhibit Idh1 Catalytic Activity and Induce Hif-1alpha." *Science* 324.5924 (2009): 261-5. Print.
Zhou, Z., et al. "Targeting Hippo Pathway by Specific Interruption of Yap-Tead Interaction Using Cyclic Yap-Like Peptides." *FASEB J* 29.2 (2015): 724-32. Print.

**CURRICULUM VITAE**

**Anthony F. Folck**

## Education

2016 M.S., Biochemistry and Molecular Biology, Indiana University, Indianapolis, IN

2014 B.S., Cellular, Molecular & Developmental Biology, Purdue University, West Lafayette, IN

## Academic Honors

2013 Dean's List, Purdue University, West Lafayette, IN

2013 National Chapter-Scholar Award, Kappa Sigma, Purdue University, West Lafayette, IN

## Experience

2014 – 2016 Molecular Biology and Biochemical Research, Laboratory of Clark Wells, Indiana University School of Medicine, Indianapolis, IN

2015 Commercial Training & Development, Genentech Inc., South San Francisco, CA

2013 Biomedical Research, Microfluidics Innovations, West Lafayette, IN

2013 Cancer Biology and Patient Tailoring, Eli Lilly & Co., Indianapolis, IN

2011-2013 Genetic and Molecular Research, Purdue University, West Lafayette, IN